

EM ice thickness measurements during 2004 IRIS field campaign

February 05 to March 17, 2004



Christian Haas, AWI
With contributions from the IRIS 2004 field party

May 2004

**EM ice thickness measurements during 2004 IRIS field campaign, February 05 to
March 17, 2004**

Christian Haas, AWI

Executive summary	3
1. Introduction	4
1.1 Ice conditions during the field campaign	5
2. Ground measurements	7
2.1 Long profile across fast ice edge	7
2.2 Drifting ice floe profile	10
3. Helicopter measurements	12
3.1 Processing	13
3.2 EM modelling	13
3.2.1 Deep water	14
3.2.2 Shallow water under fast ice	14
3.3 Results	15
3.3.1. Comparison of measurements over long fast ice profile	15
3.3.1 Grid and triangle flights	17
3.4 Profile plots	22
05.2.2004 Grid	23
05.2.2004 Triangle	25
09.2.2004 Grid	27
10.2.2004 Triangle	29
11.2.2004 Grid	31
18.2.2004 Grid	33
18.2.2004 Triangle	35
20.2.2004 Triangle	37
23.2.2004 Triangle	39
23.2.2004 Grid	41
29.2.2004 Triangle	43
29.2.2004 Grid	45
01.3.2004 Grid	47
04.3.2004 modified Triangle	49
05.3.2004 Grid	51
14.3.2004 Grid	53
14.3.2004 Triangle	55
14.3.2004 2 legs for ASIRAS	57
17.3.2004 ASIRAS fast ice profile	58

Executive summary

This report summarizes all airborne and ground-based ice thickness measurements performed during the IRIS 2004 field campaign, February 5 to March 17, and presents the main results. In total, 17 flights were performed in the eastern Bay of Bothnia off Marjaniemi. They covered the main ice regimes in the area, and document well changes of the thickness distribution in response to ice dynamics, in particular during a major deformation event on February 29. The data show a large number of different thickness classes representative of different growth phases. Ground based activities with contributions from all project partners achieved a 3380 m long drill-hole and EM thickness profile, providing a unique opportunity for the validation of EM measurements over level and deformed ice. Results suggest that EM data of deformed ice > 1 m thick need to be multiplied by a factor of 2.4 to agree with the drill-hole thicknesses. The report also serves as an introduction for user of the thickness data which are all publicly available on AWI's IRIS internet site at

<http://www.awi-bremerhaven.de/Modelling/SEAICE/IRIS>.

1. Introduction

The main objective of the IRIS project is the quantitative derivation of the amount of ridges from satellite imagery and their prediction by means of numerical models. The information is needed to further improve ice information for shipping, as e.g. provided by national ice services.

For the development of remote sensing algorithms and model parameterisations, as well as for model validation, the workplan had foreseen a major extensive field campaign in 2004 for the acquisition of in-situ ice thickness and surface roughness data. This was part of WP2 (Baltic field studies). Helicopter-borne EM (HEM) measurements were performed between February 05 and March 17, 2004, with an extensive ground validation period between February 22 and March 6. For the latter, all IRIS partners had sent some scientists to support the measurements (FIMR, HUT, KMY, SAMS, SMHI). The AWI team consisted of 5 people (Wolfgang Dierking, Sibylle Goebell, Christian Haas, Torge Martin, and Andreas Pfaffling).

The measurement systems and field plan were described in IRIS deliverables 1 and 9, the Baltic Field Plan and Thickness Distributions from 1st field phase. The 2004 measurements were all performed in the Bay of Bothnia, using the Finish research station at Marjanemi, Hailuoto, as a base (Figure 1). The goal of the extended airborne campaign was to observe temporal changes of the sea ice thickness and ridge distributions in response to ice dynamics. The latter was observed by means of drifting buoys deployed on the ice, which transmitted their 3-hourly positions via the ARGOS satellite system. Buoy tracks between February 26 and March 15 are also shown in the Map (Figure 1). Unfortunately, due to technical problems, measurements could not be started earlier with the beginning of thickness surveys.

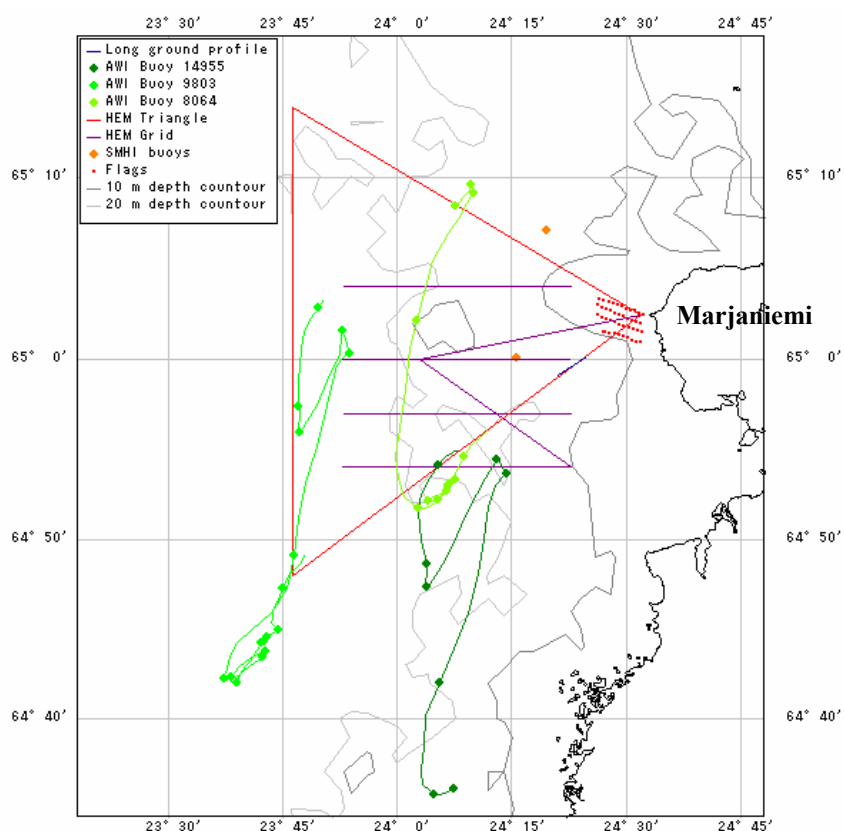


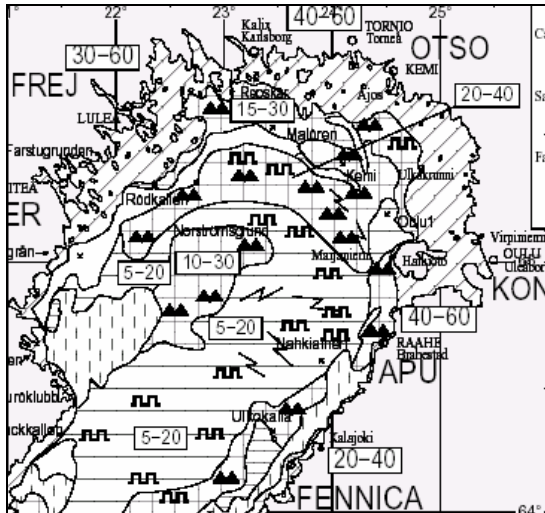
Figure 1: Map of IRIS 2004 study area in the Bay of Bothnia, west off the island of Hailuoto. EM flight tracks, the location of the 3.38 km ground profile, as well as real-time drift trajectories of three buoys are shown.

1.1 Ice conditions during the field campaign

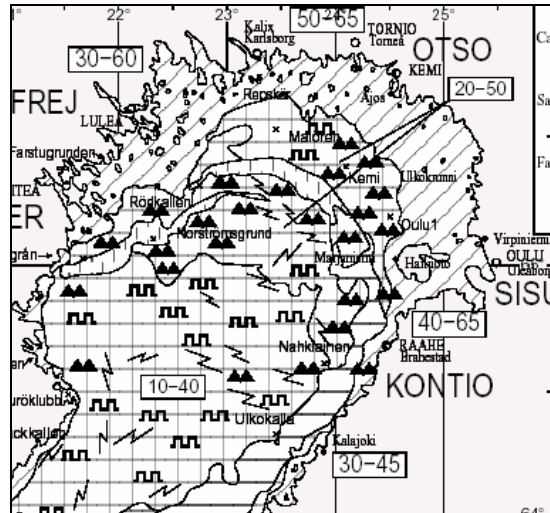
The ice season of 2004 was very mild, with ice formation starting only in late December in the Bay of Bothnia. In the southern Bay of Bothnia, only thin rafted ice was present throughout the winter, while the Gulf of Bothnia remained almost ice free. The study region to the northwest and southwest therefore consisted of thick ridged ice in the North and East, and of thinner rafted ice in the South. This is well represented in the thickness data presented below.

Figure 2 shows typical ice conditions during the study period, while Figure 1 shows ice dynamics after February 26. After that date, ice conditions were dominated by southerly ice drift opening up large polynyas in the study region, in particular along the fast ice edge southwest of Hailuoto. These open water and thin ice areas are well visible in the thickness profiles as well. On February 29, strong southerly winds moved the ice back northwards, resulting in rafting of most ice formed in the polynya in the meantime. This event is well represented in the ice chart of March 02. During the following 4 days, the ice moved southward again, opening up even larger polynyas which started to freeze up afterwards. Later then, there was some ice movement back and forth, without changing overall ice conditions any more. Note that the northernmost buoy (ID 8060) started moving only after the strong storm on February 29, while the southernmost buoy (ID 14955) remained stationary after March 5.

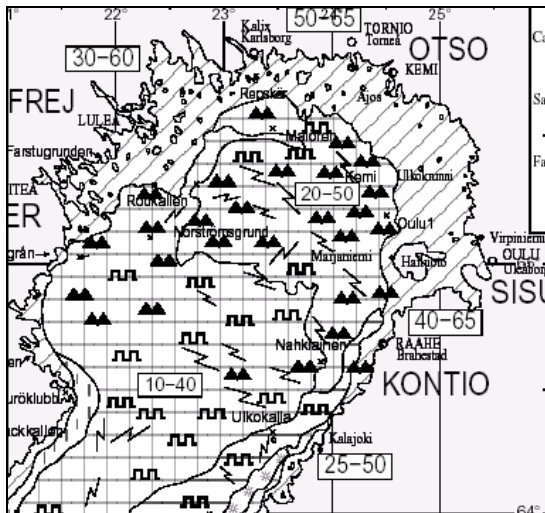
Meteorological data from Hailuoto and some other stations around the Bay of Bothnia is available on request from FIMR.



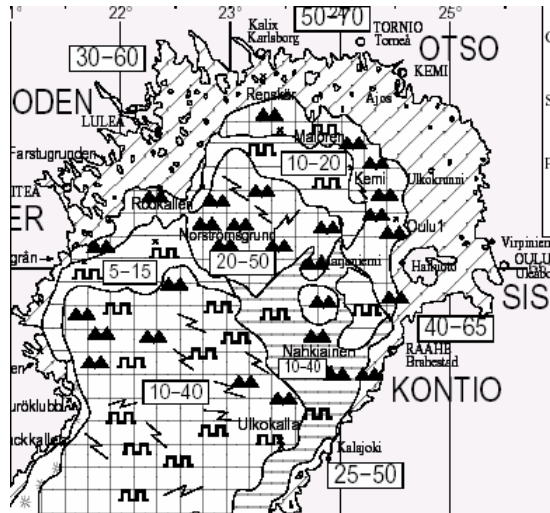
5.2.2004



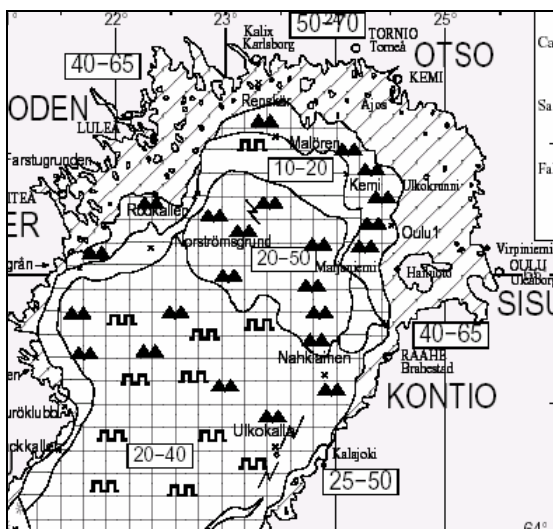
29.2.2004



2.3.2004



5.3.2004



14.3.2004

Figure 2: Ice conditions during the field campaign. The Feb.29 and March 02 charts show changes due to the deformation event. Ice charts kindly provided by Finish Ice Service, FIMR.

2. Ground measurements

The goal of the ground validation campaign was to provide data on ridge shape and volume, as well as for the validation of EM data. A 3280 m long line was profiled by means of drill-hole and EM snow and ice thickness measurements and freeboard surveying. The profile was coincident with the third leg of the HEM triangle flight (see Fig. 1 and Section 3), and extended across the old fast ice edge, which was moved further out to sea after the deformation event on February 29 (see Sect. 1.1). Another 1 km profile was surveyed on a drifting ice floe further out on that HEM profile leg. While all EM measurements and the surveying have been performed with a point spacing of 5 m, drill-hole spacing was very variable ranging between 5 to 50 m. Only by these means it was possible to obtain such a long profile, with the EM data providing higher spatial resolution than the drill-hole measurements supporting the EM soundings.

A Geonics EM31 induction sounder was used for the ground-based EM measurements (Kovacs and Morey, 1992¹; Haas et al., 1997²). The instrument was laid onto the snow surface and operated in horizontal dipole mode (HDM). Ice thickness was computed from the measured apparent conductivity by means of a negative exponential transformation equation derived from regression of a 1D model curve (Fig. 3). For the model, a salinity of 3.4 ppt was used which was a mean value of several measurements performed with a salinometer.

2.1 Long profile across fast ice edge

Figure 4 shows the long thickness profile on the fast ice SW of Marjaniemi obtained as described above. From both Figures (3 & 4) it can be seen that level ice thickness is well determined by the EM measurements, but that deformed, thick ice thickness is strongly underestimated. A regression to the drill-hole data (Figure 3) was not used for the thickness inversion because too many EM soundings would have yielded no result due to negative arguments of the logarithms in the transformation equation.

To further investigate the disagreement between EM and drill-hole results, EM thicknesses derived from inversion of a model equation and drill-hole thicknesses are compared in Figure 5. Two linear regressions have been performed for thicknesses below and above 1 m, a value chosen arbitrarily based on visual inspection of the data. The agreement between EM and drill-hole data below 1 m is very good, with an intercept and slope of almost 0 and 1, respectively, and a correlation coefficient of $r = 0.89$. Above 1 m, ice thickness is underestimated by as much as a factor of 2.5 (slope = 0.41). This is remarkably similar to the results of Haas and Jochmann (2003)³ obtained from measurements on a nearby lighthouse. However, the correlation is quite good, with $r = 0.83$.

¹ Kovacs, A., and R. M. Morey, Sounding sea-ice thickness using a portable electromagnetic induction instrument, *Geophysics*, 56, 1992-1998, 1991.

² Haas, C., S. Gerland, H. Eicken, and H. Miller, Comparison of sea-ice thickness measurements under summer and winter conditions in the Arctic using a small electromagnetic induction device, *Geophysics*, 62, 749-757, 1997.

³ Haas, C., and P. Jochmann, Continuous EM and ULS thickness profiling in support of ice force measurements, in Proceedings of the 17th International Conference on Port and Ocean Engineering under Arctic Conditions, POAC '03, Trondheim, Norway, edited by S. Loeset, B. Bonnemaire, and M. Bjerkas, Department of Civil and Transport Engineering, Norwegian University of Science and Technology NTNU, Trondheim, Norway, Vol. 2, 849-856, 2003.

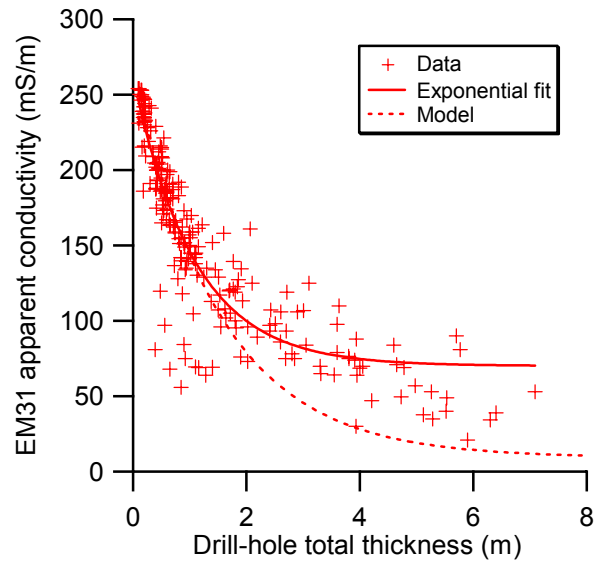


Figure 3: Comparison of EM31 conductivity readings with ice thickness (snow+ice) determined in coincident drill holes. Lines show a negative exponential regression to the data as well as a 1D model curve using a sea water salinity of 3.4 ppt.

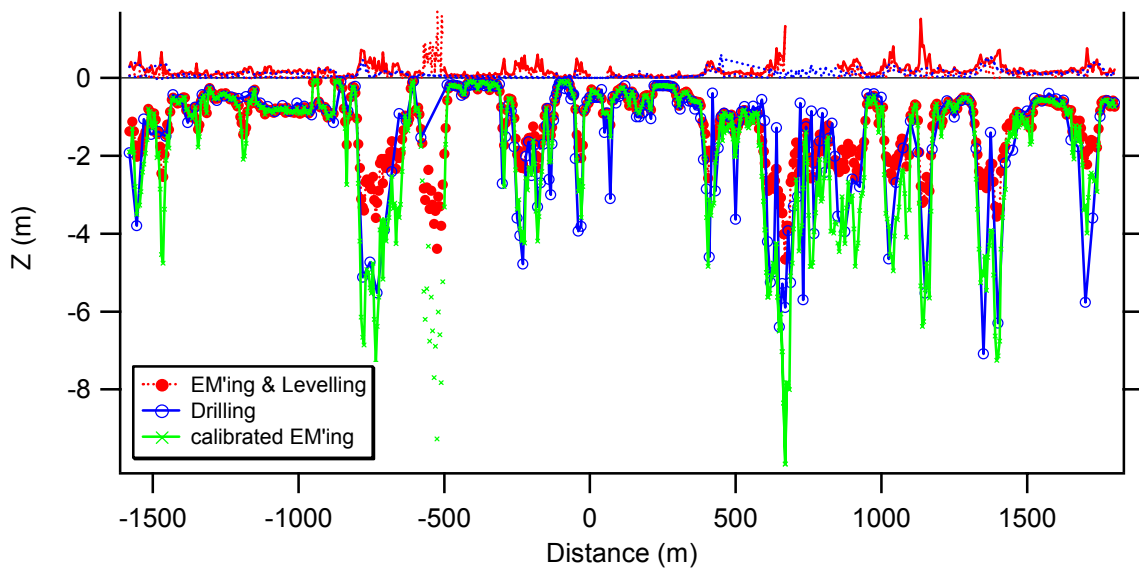


Figure 4: Thickness profile of the long line with a lateral point spacing of 5 m. The fast ice edge before the deformation event was at 0 m, the newly deformed ice is to the left (negative distance). Freeboard and surface elevation were obtained by surveying and ruler stick measurements. EM thickness was obtained from inverting a model curve. Corrected EM thickness was obtained using equations presented in Figure 5. Spacing of drill-hole data is variable, ranging between 5 and 50 m.

The equations shown in Figure 5 provide a means to correct the EM data over deformed ice. This is demonstrated in Figure 6, where a good agreement can be seen between drill-hole and corrected EM data, and where the EM data provide accurate information at locations where drilling would have been too slow and tedious. Table 1 summarizes all thickness results, showing that the corrected mean EM thickness is actually 0.45 m larger than the drill-hole thickness, which is due to the fact that there are 3.2 times more EM data mainly over ridged ice than there are drill-hole data. However, as can be seen in Figure 6, the dominant modal

thicknesses are very well represented in all data sets. It should be noted that the ground measurements show that there were a lot of different level ice classes representing different developmental stages of the ice. This is confirmed by the airborne data below. Table 1 also summarizes results of the snow thickness measurements and laser surveying. The corresponding snow thickness and surface elevation distributions are shown in Figure 7.

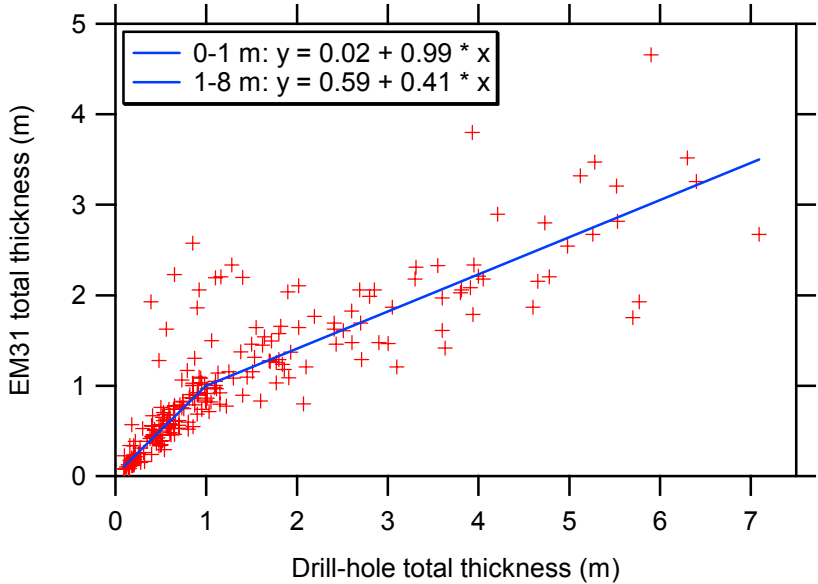


Figure 5: Comparison of EM31 and drill-hole derived thickness measurements carried out at coincident locations. Lines and equations show linear regressions for ice thicknesses below and above 1 m.

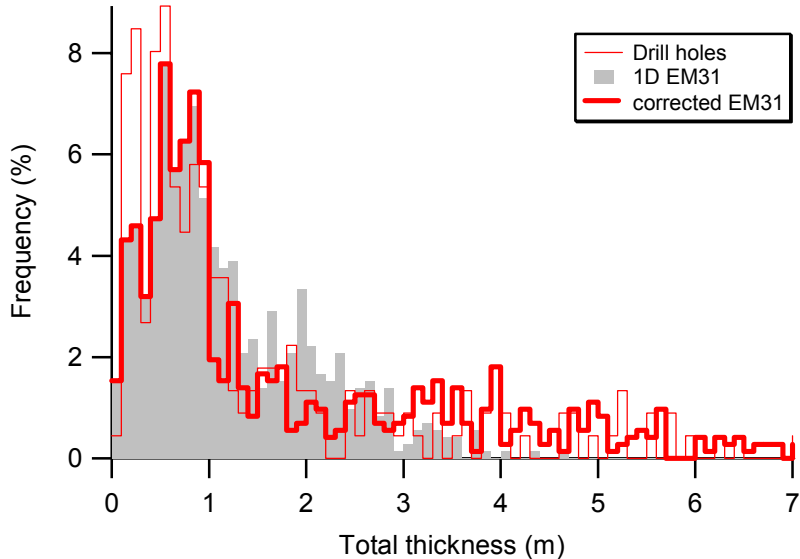


Figure 6: Thickness distributions obtained by drilling and EM sounding using a 1D model for thickness inversion. The thick line shows the corresponding distribution for the corrected EM data (cf. Fig. 5.). Note that the number of EM data is 3.2 times larger than the number of drill-hole data (cf. Table 1).

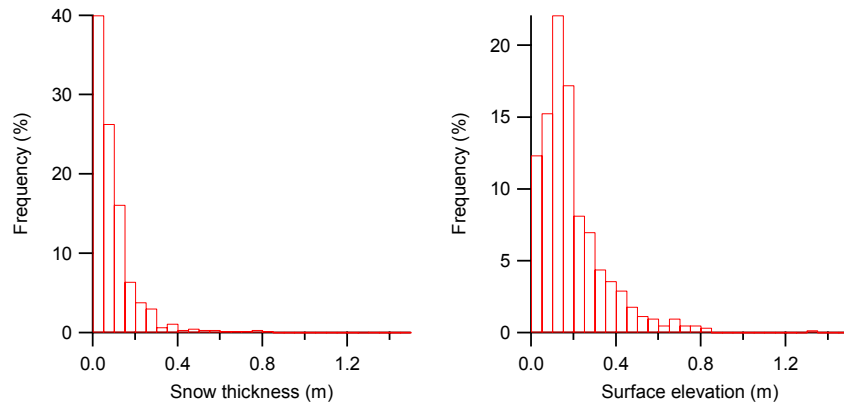


Figure 7: Histograms of snow thickness and surface elevation (snow surface height above water level) obtained from ruler measurements and surveying along the long fast ice profile (cf. Table 1).

Table 1: Summary of ground-based thickness measurements (cf. Figs. 4-10).

	Long fast ice profile		Drifting floe profile	
		N		N
Mean drill hole thickness	1.46±1.52 m	224	n.a.	23
Mean EM thickness	1.25±0.89 m	719	1.19±0.83 m	201
Mean corrected EM thickness	1.91±1.89 m	719	1.80±1.70 m	201
Drill-hole modes	0.2, 0.5, 0.8, 1.8 m	224	n.a.	23
EM modes	0.2, 0.5, 0.8, 1.6, 1.9 m	719	0.3, 0.7, 1.2, 1.4, 1.8 m	201
Corrected EM modes	0.2, 0.5, 0.8, 1.2, 1.7 m	719	0.3, 0.7, 0.9, 1.1, 1.4, 1.9 m	201
Mean snow thickness	0.09±0.12 m		0.11 m	
Modal snow thickness	0.00-0.05 m	628	0.00-0.05 m	71
Mean surface elevation	0.19±0.17 m		0.28±0.19 m	
Modal surface elevation	0.10-0.15 m	616	0.15-0.20, 0.25-0.3 m	71

2.2 Drifting ice floe profile

On February 28, an ice floe at 64.79°N, 24.06°E was visited by helicopter. Unfortunately, due to deteriorating weather conditions, drill-hole measurements and surveying had to be stopped before they were finished.

Figure 8 shows the thickness profile of the floe. The corresponding thickness distributions are presented in Figures 9&10, and the results are summarized in Table 1. It is noteworthy that the results of both profiles are quite similar, considering that the accuracy of the EM measurements is only about 0.1 m.

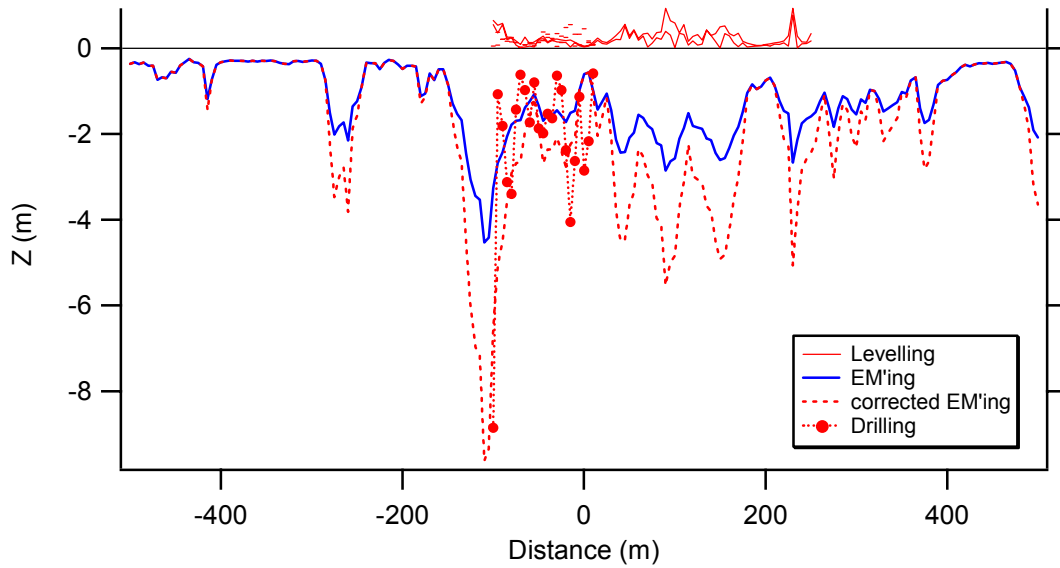


Figure 8: Thickness profile of the drifting ice floe with a lateral point spacing of 5 m. 0 m refers to the helicopter landing site, with positive distance towards 240°. Freeboard and surface elevation were obtained by surveying and ruler stick measurements. EM thickness was obtained from inverting a model curve. Corrected EM thickness was obtained using equations presented in Figure 5.

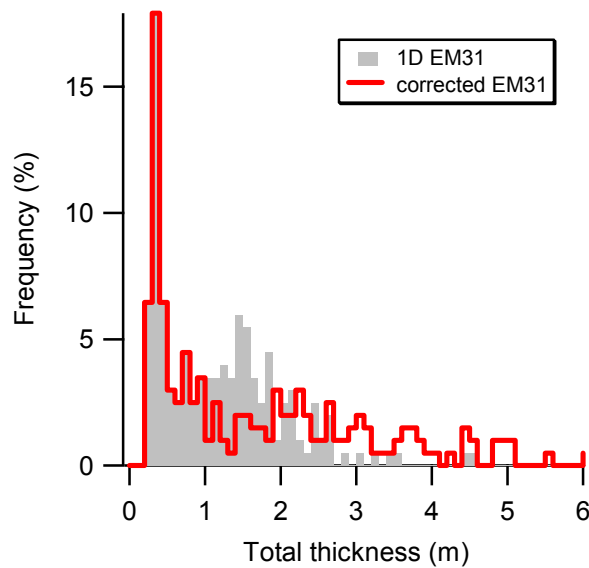


Figure 9: EM thickness distribution obtained by EM sounding using a 1D model for thickness inversion. The thick line shows the corresponding distribution for the corrected EM data (cf. Fig. 5).

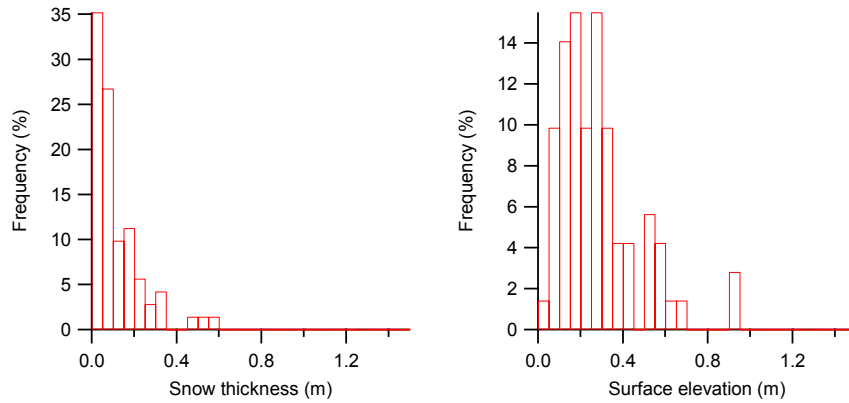


Figure 10: Histograms of snow thickness and surface elevation (snow surface height above water level) obtained from ruler measurements and surveying along the long fast ice profile (cf. Table 1).

3. Helicopter measurements

In total, 17 HEM thickness flights have been performed between February 5 and March 14, with two additional flights on March 14 and 17 in support of a CryoSat validation flight of an AWI aircraft. Flights were performed following two main profile patterns (Fig. 1):

1. A grid pattern with four 15 nautical miles long E-W profiles and two diagonals inbetween.
2. A triangle with 25 nautical miles side length.

Dates and results of those flights are summarized in Table 2. All flights were performed with a ground speed of 60 knts. With an EM sampling rate of 10 Hz, this corresponds to a measurement point spacing of ca 3 m. However, it should be noted that the actual spatial resolution of the measurements is only 20 to 30 m.

Table 2: Summary of results of all HEM flights (cf. Fig. 1). Open water (OW) fraction was computed by summing all thicknesses in a range between -0.1 to +0.1 m. Note that the mode is the maximum of each thickness distribution, and that there were many secondary modes in each thickness distribution (cf. Fig. 18 and plots in Sect. 3.4).

Date	Grid			Triangle		
	Mode (m)	Mean±sdev (m)	OW fraction (%)	Mode (m)	Mean±sdev (m)	OW fraction (%)
05.02.2004	0.4	1.17±0.85	5.04	0.3	1.13±0.76	7.21
09.02.2004	0.2	0.98±0.80	11.65			
10.02.2004				0.3	0.85±0.72	13.54
11.02.2004	0.3	0.91±0.70	10.78			
18.02.2004	0.2	1.09±0.93	13.38	0.4	1.07±0.76	7.75
20.02.2004				0.2	0.98±0.75	11.65
23.02.2004	0.1	1.04±0.91	13.41	0.2	0.87±0.75	12.48
29.02.2004	0.2	0.93±0.89	17.72	0.1	1.04±0.83	15.00
01.03.2004	0.6	1.28±0.94	5.56			
04.03.2004				0.0	0.95±0.94	23.86
05.03.2004	0.1	1.04±0.98	24.98			
14.03.2004	0.1	0.98±0.96	20.70	0.2	1.36±0.99	6.68

3.1 Processing

Data processing was performed as described in the Data Report for the 2003 measurements (IRIS Deliverable 9). The main steps were again drift compensation, calibration for ice thickness zero over open water leads, and thickness computation and editing. As in 2003, only measurements performed below an altitude of 20 m were considered reliable.

However, data presented here and released to the project partners were additionally smoothed with a binomial filter to reduce noise. This is demonstrated in Figure 11, showing that the filter does not remove any of the main ice thickness information. Filtering is also well possible because the point spacing of the HEM measurements is much smaller than their spatial resolution.

Comparison of results obtained from the four available channels (Inphase and Quadrature of f1 (3.6 kHz) and f2 (112 kHz)) showed that in 2004 after some changes to the EM system Quad(f2) yielded by far the best results and was even not affected by shallow water below the fast ice. Therefore, only the Quad(f2) data are released here. The observation is also confirmed by the model results shown in Figures 12&13. The model also shows that f2 should actually give the best results. However, there are still some technical problems with this high frequency leading to variable signal drift, so that we considered them as less reliable.

The open water fraction (Table 2) was computed summing all thicknesses in a range between -0.1 to +0.1 m.

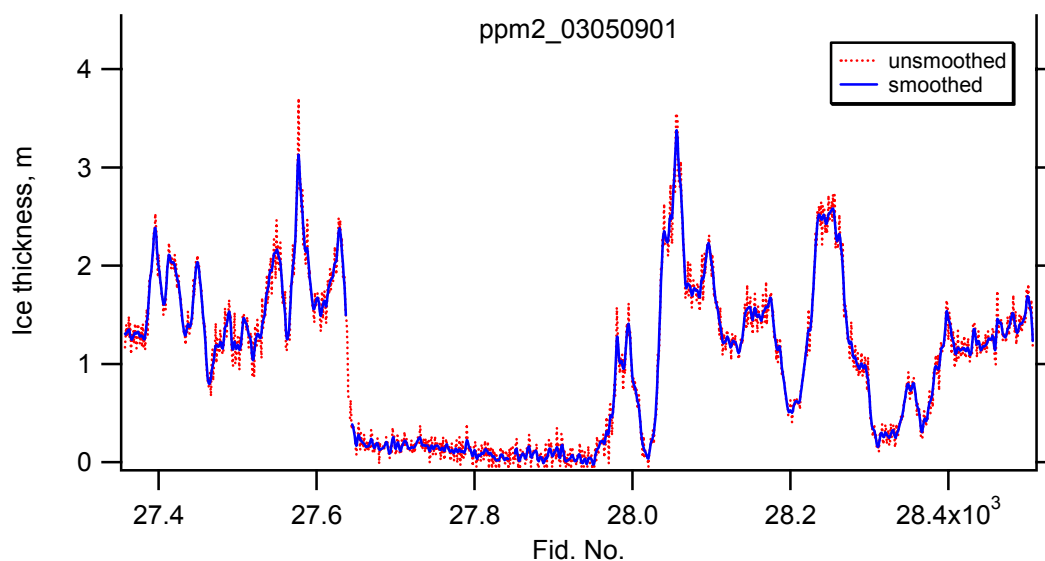


Figure 11: Typical thickness profile (from 3rd leg of grid on March 05) with raw and smoothed data, using a binomial filter. The filter only removed noise without affecting the ice thickness information.

3.2 EM modelling

Brackish Baltic Sea water poses a challenge for EM ice thickness measurements due to its low salinity, which was measured to be 3.4 ppt west off Hailuoto, corresponding to a seawater conductivity of about 340 mS/m (compared to 2400-2700 in the Arctic Ocean). The EM response of a layered underground can well be computed by numerical modelling. Here, the response about deep water is presented, as well as the sensitivity of our EM bird to shallow water underneath the sea ice.

For the modelling, the AWI EM bird instrument parameters have been taken into account, i.e. a frequency of 3680 Hz and coil spacing of 2.77 m for f1, and a frequency of 112000 Hz and a coil spacing of 2.05 m for f2.

3.2.1 Deep water

Figure 12 shows the EM response over infinitely deep water with a conductivity of 340 mS/m for varying bird heights above the water surface. The well-known negative-exponential decrease with increasing bird height can be seen. Contrary to high conductivity sea water of the Arctic, the strongest signal results from measurements of the Inphase of f2, corresponding to our observations, while Quad(f2) is very small. Also contrary to the Arctic, Quad(f1) is larger than Inph(f1) for heights below approximately 15 m. This justifies our decision to use ice thicknesses derived from Quad(f1) as the final product for the IRIS partners.

The negative exponential decrease with bird height shows the importance of considering height with judging the measurement's accuracy. For example, from the data shown in Figure 12 the gradient of Quad(f1) is about 15 ppm per 0.1 m thickness change at 10 m bird height, and 5 ppm per 0.1 m thickness change at 15 m height. Here, a thickness change is equivalent to a height change, because like air ice is considered to have zero conductivity. With the present noise level of about 10 ppm, this means that thickness changes of 0.1 m can only be resolved with flight heights close to 10 m. However, with the applied smoothing the noise level is reduced to about 5 ppm. Therefore, our assumption that thickness changes of 0.1 m can be resolved with our bird even with low seawater conductivities of 340 mS/m is justified for the bird altitudes chosen for the IRIS flights (12-14 m).

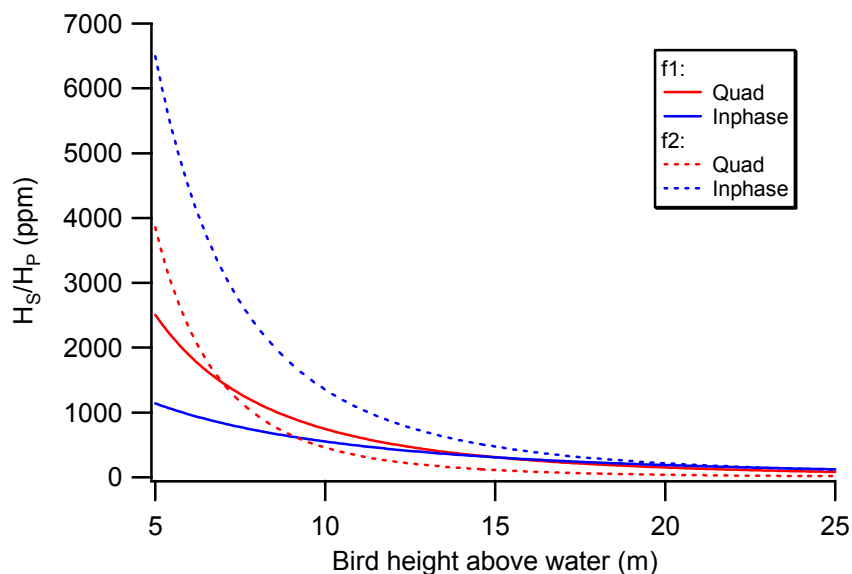


Figure 12: EM response for different bird heights above sea water with a conductivity of 340 mS/m. f1: 3680 Hz, 2.77 m coil spacing; f2: 112000Hz, 2.05 m coil spacing.

3.2.2 Shallow water under fast ice

One major problem during the IRIS 2003 and 2004 measurements was the determination of fast ice thickness over shallow water. Over shallow water, the basic assumption of our thickness inversion of a uniform halfspace with constant water conductivity is not valid. The bird actually also generates a signal in the seabed under the water. This results in a different

sensed field strength compared to the uniform half space, leading to wrong thickness estimates. The effect is larger for smaller water conductivities.

Figure 13 shows the bird response over shallow water of varying depth over a seabed of 0.1 mS/m conductivity. This is a worst case scenario, as true seabed conductivities are probably much higher, and therefore the actual bird response will be smaller. F1 shows a strong sensitivity on water depth up to depths of about 15 m. For deeper water, the seabed cannot be sensed any more. However, The Inphase and Quadrature components behave differently. Inph(f1) approaches the uniform halfspace response monotonically, whereas Quad(f1) has some local maximum inbetween (Fig. 13, left). This means that the Quadrature response is close to the halfspace response for shallower water depths than the Inphase component. However, the local response maximum at depths at about 10 m results in an underestimation of the true ice thickness. For example, at 10 m bird height, the maximum underestimation amounts to 0.35 m (corresponding to a signal difference of 56 ppm), and to an underestimation of 0.8 m at 15 m bird height. However, for water depths larger than 10 m the errors are much smaller. Both, data and model results show that Quad (f1) is much less sensitive to shallow water depth below 10 m than Inph(f1).

F2 is sensitive to water depth only for very shallow water less than 5 m deep (Fig. 13, right). The good agreement between Quad(f1) and Inph(f1) in or data therefore suggests that also the distributed Quad(f1) data are sufficiently accurate even over shallow water.

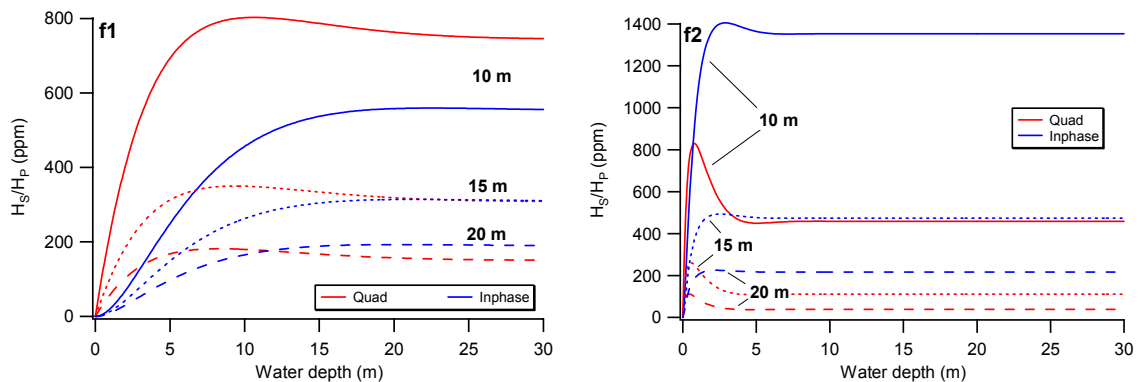


Figure 13: EM response for different water depths and bird heights of 10, 15, and 20 m above sea water with a conductivity of 340 mS/m, and with a seafloor conductivity of 0.1 mS/m. Left: f1; 3680 Hz, 2.77 m coil spacing. Right: f2; 112000Hz, 2.05 m coil spacing.

3.3 Results

3.3.1. Comparison of measurements over long fast ice profile

The IRIS 2004 measurements provided the unique opportunity for validation of the HEM measurements over a long ground profile. The ground profile was overflown six times, twice on February 29 before the deformation event, and twice on March 4 and 14. Because the February 29 measurements consist only of half the ground line (the rest was open water and new ice in the coastal polynya), only the March measurements were used in the following analysis.

In order to synchronize the HEM measurements, they were just plotted against their GPS longitudes (Fig. 14). By means of event markers put into the HEM data during the overflight and by means of video footage (Fig. 15), some significant points of the ground profile were used to align the flight tracks with the ground measurements. The agreement between the spacing of the EM31 measurement points and the HEM spacing was very good except for a

short section along the new ridge, where the helicopter flight track deviated from the ground measurements. Afterwards, all data were resampled to a uniform point spacing of 5 m. Because the flight tracks along the ground line were so short, their calibration was very difficult, and indeed the main modes of the thickness distribution were offset by as much as ± 0.2 m. Therefore, the HEM thicknesses were shifted by plus or minus 0.2 m to achieve good agreement with the EM31 thicknesses. The resulting HEM profiles were averaged to yield a mean HEM thickness. This is presented in Figure 16. The corresponding histograms are shown in Figure 17, and Table 3 lists the main statistics of both data sets.

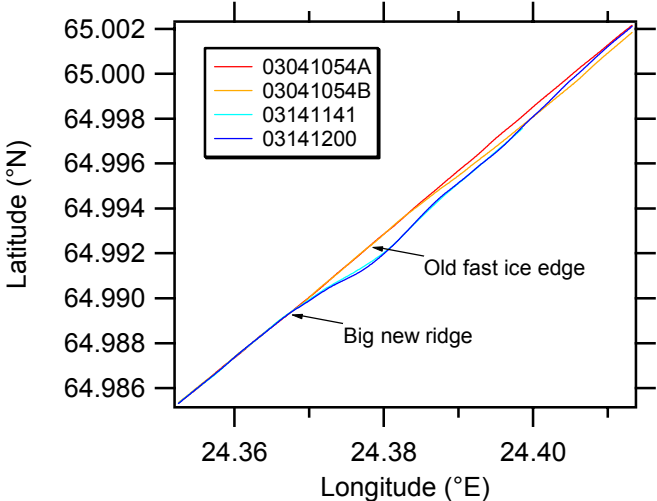


Figure 14: Map of HEM flight tracks along fast ice ground profile.



Figure 15: Photographs obtained from nadir video camera showing varying agreement between HEM flight track and ground profile (visible by footsteps in the snow).

Table 3: Summary of mean HEM and smoothed EM31 measurements over long fast ice profile (cf. Fig. 16)

	Mean HEM profile	Mean EM31 ground profile
Mean thickness	1.25 \pm 0.92 m	1.21 \pm 0.83 m
Modal thickness	0.1, 0.5, 0.7, 1.8 m	0.1, 0.5, 0.8, 1.9 m

Again, as with the comparison with the drill-hole data (Table 1), there is very good agreement between the data sets, and in fact the HEM data provides the same information as the EM31 measurements. This is quite remarkable given the different footprints of the measurements, and the fact that the HEM lines were not always exactly coincident with the EM31 profile (see Fig. 15). As suggested by the results of the drill-hole measurements, thicknesses above 1 m should be corrected using the equation in Figure 5 to obtain the best agreement with the drill-hole data.

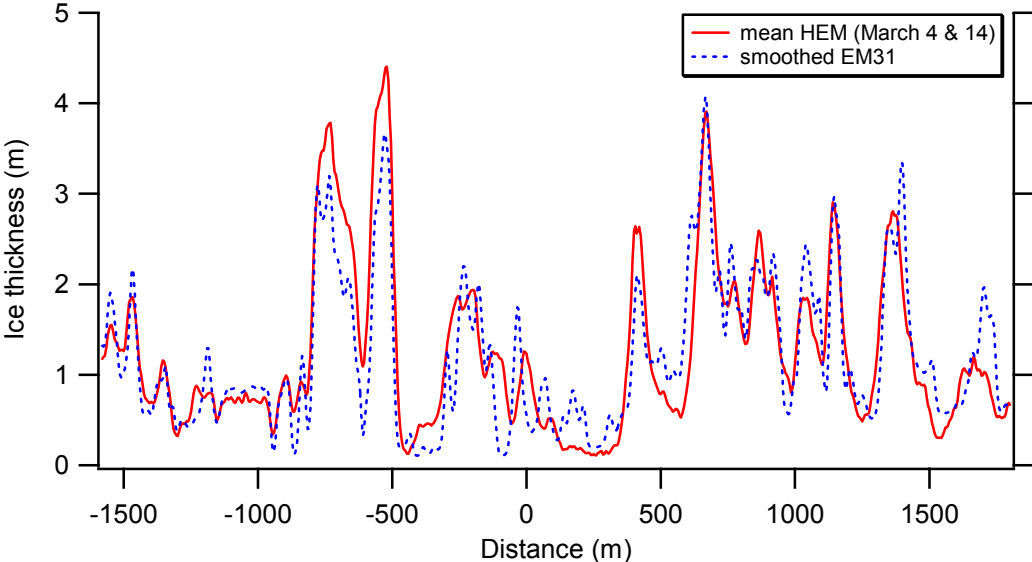


Figure 16: Mean HEM and smoothed EM31 thickness profiles along fast ice line (cf. Fig. 14).

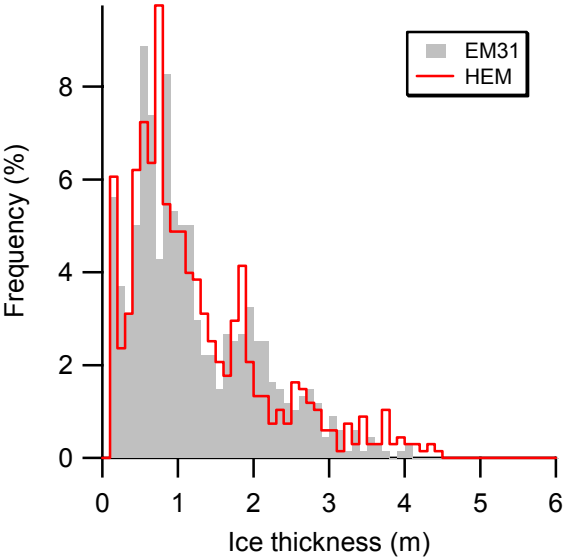


Figure 17: HEM and EM31 Thickness distributions of long fast ice profile (cf. Fig. 16).

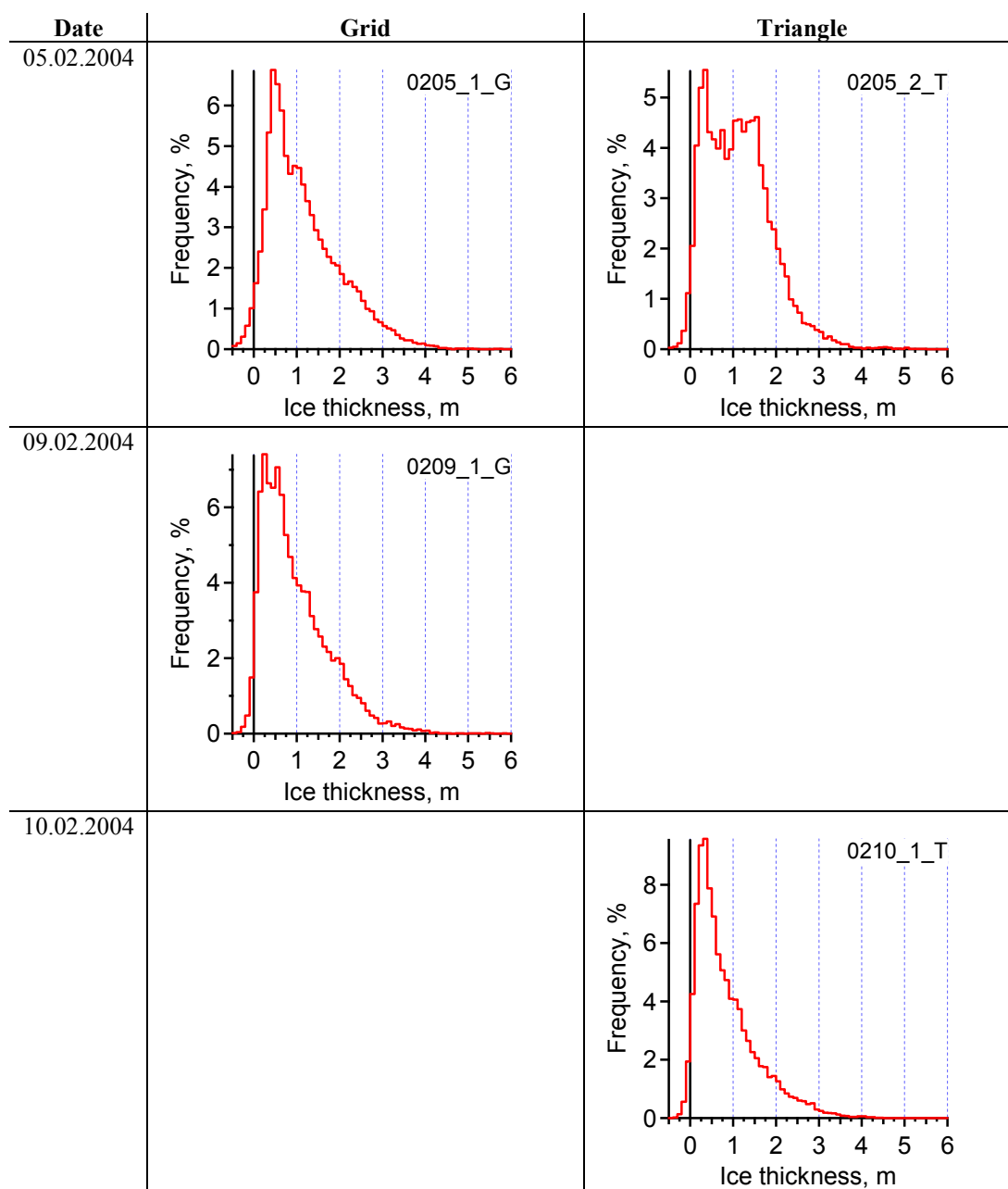
3.3.1 Grid and triangle flights

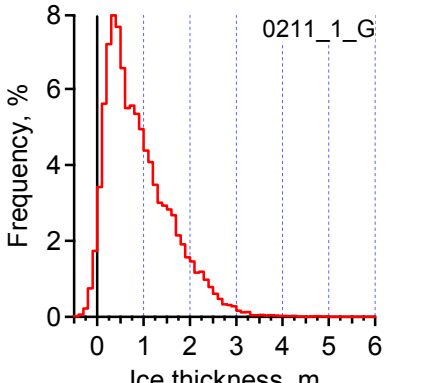
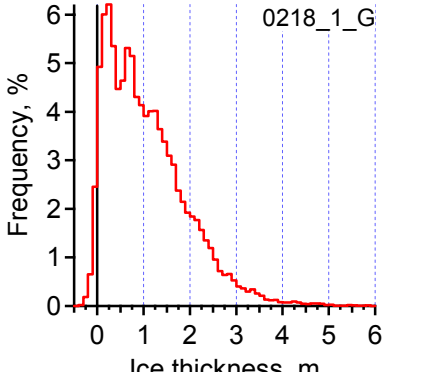
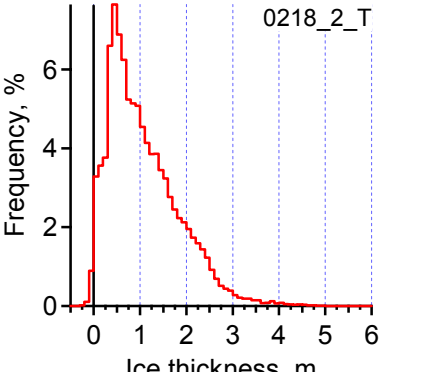
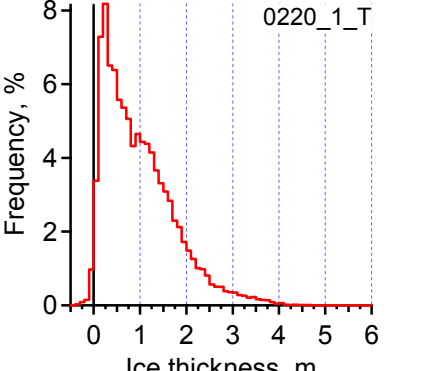
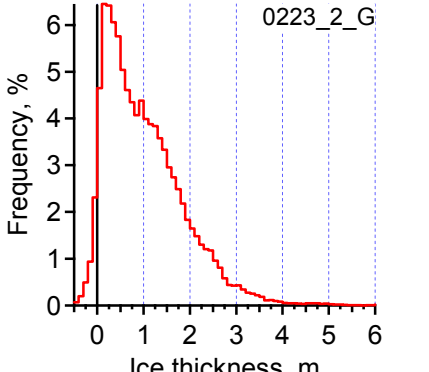
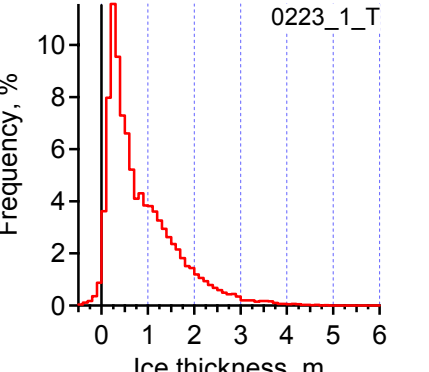
The results of the surveys along the grid and triangle lines are summarized in Table 2 and in the thickness profiles and histograms of each leg plotted in Section 3.4. Figure 18 summarizes the histograms for every flight. The data shows clearly

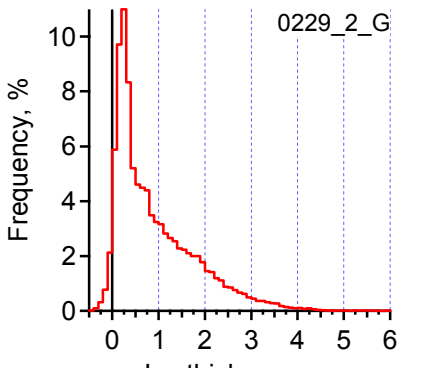
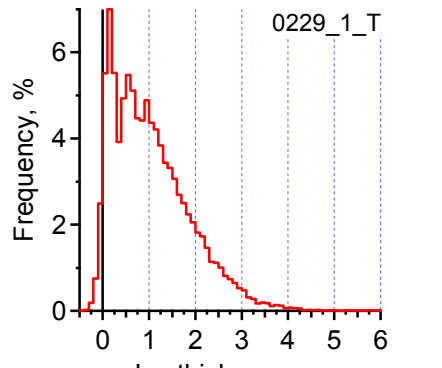
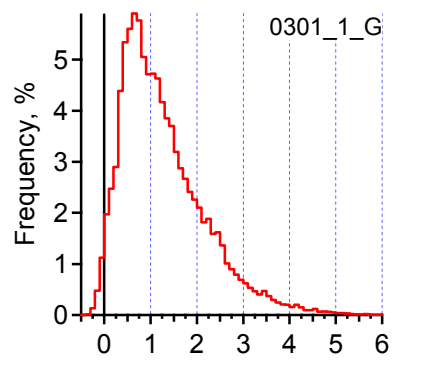
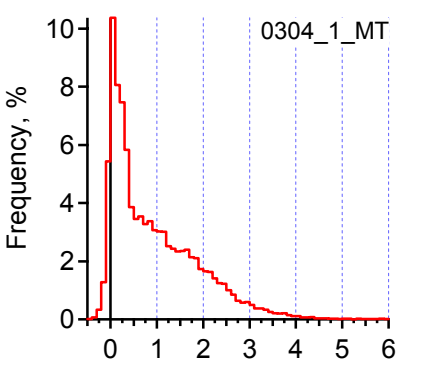
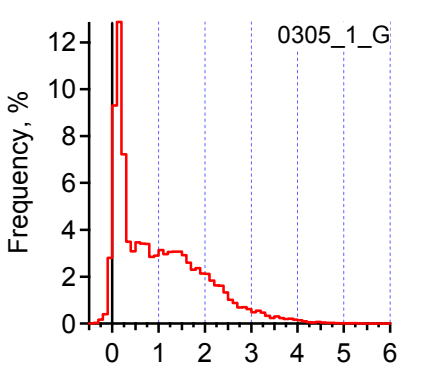
- that there was thicker ice in the North than in the South,

- that there were many different thickness classes in the area, many exceeding a thickness of 1 m,
- that the amount of open water and thin ice increased in accordance with the buoy drift measurements (Fig. 1),
- and that the deformation event removed all thin ice and lead to large amounts of deformed ice in the area.

However, the relationship between buoy drift/ice divergence and mean ice thickness is not always straightforward (except for e.g. a comparison of ice thicknesses between February 29 and March 5) and a more careful analysis involving also model simulations is required. One reason obscuring a clear divergence signal in the thickness data is that the observations were not in a Lagrangean reference frame. Therefore, the data is subject to advection of different ice classes into the measurement area. Another reason is that the ice thickness in the whole area had a strong N-S gradient, reducing the significance of a mean thickness for a whole leg.



Date	Grid	Triangle
11.02.2004	 <p>0211_1_G</p>	
18.02.2004	 <p>0218_1_G</p>	 <p>0218_2_T</p>
20.02.2004		 <p>0220_1_T</p>
23.02.2004	 <p>0223_2_G</p>	 <p>0223_1_T</p>

Date	Grid	Triangle
29.02.2004	 <p data-bbox="608 248 730 275">0229_2_G</p>	 <p data-bbox="1083 248 1206 275">0229_1_T</p>
01.03.2004	 <p data-bbox="608 658 730 685">0301_1_G</p>	
04.03.2004		 <p data-bbox="1083 1068 1206 1095">0304_1_MT</p>
05.03.2004	 <p data-bbox="608 1478 730 1505">0305_1_G</p>	

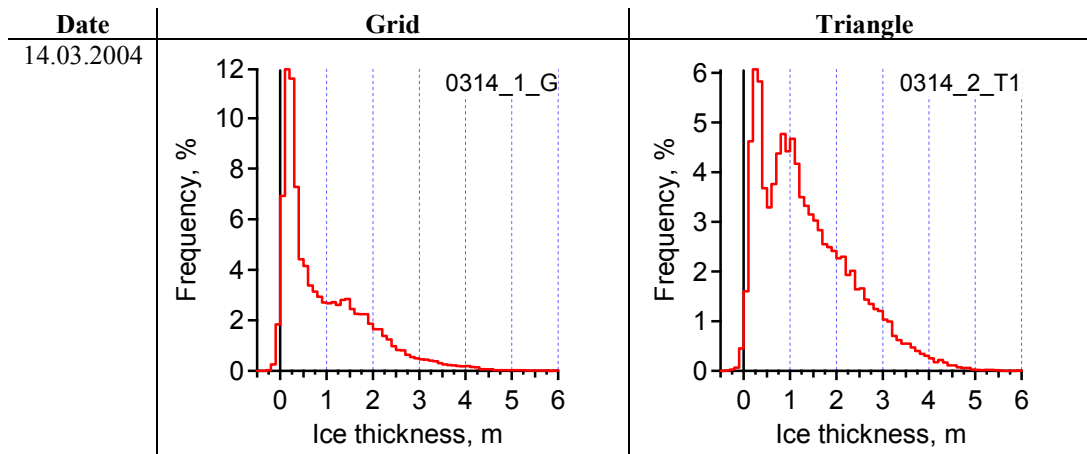


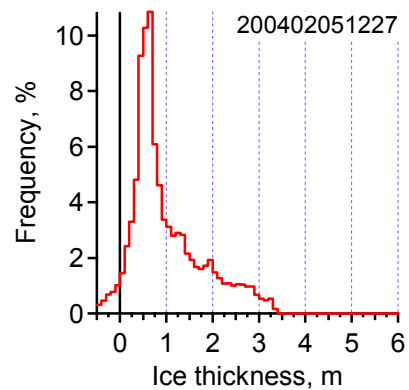
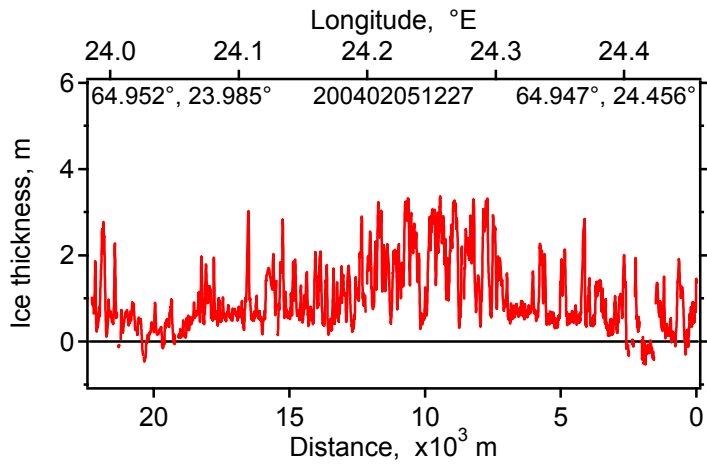
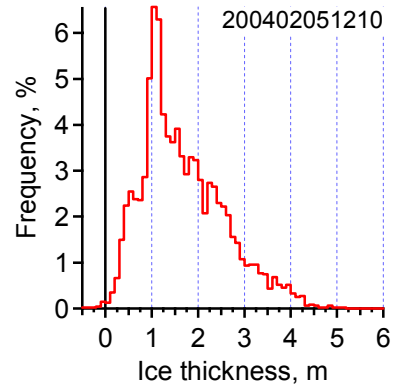
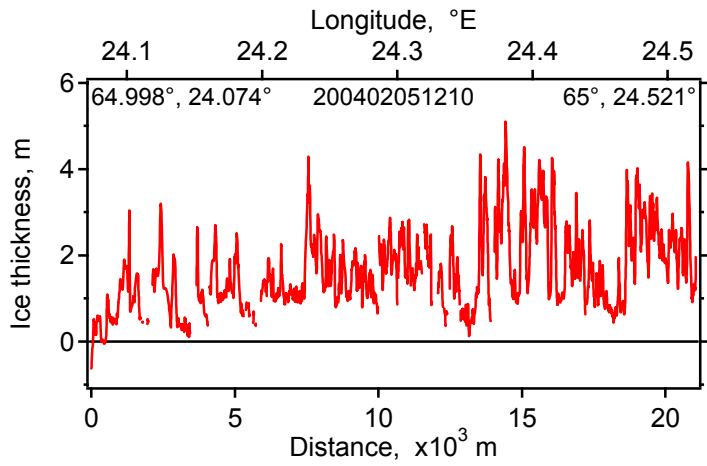
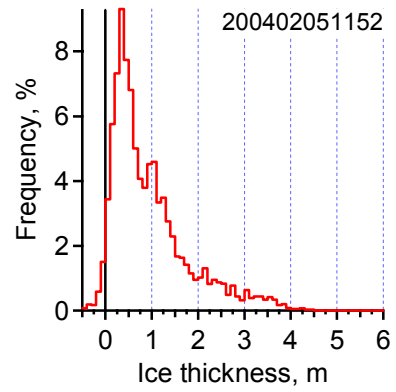
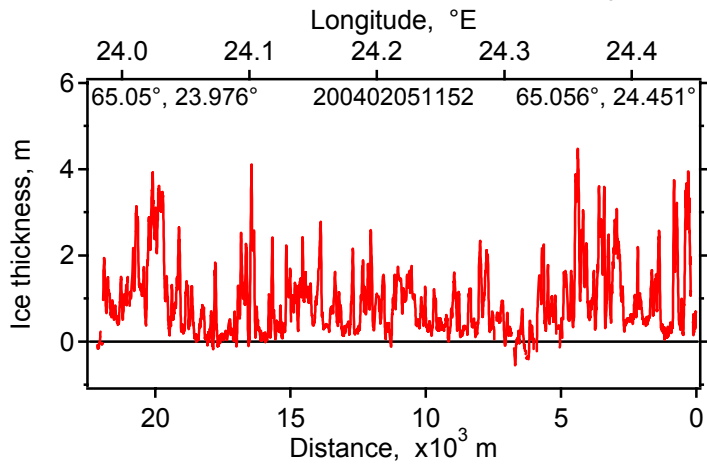
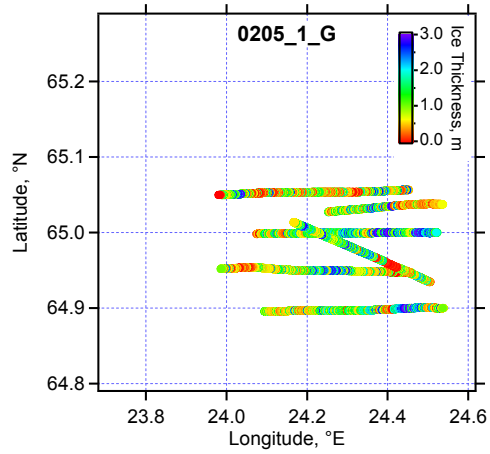
Figure 18: Thickness distributions of all IRIS 2004 flights (cf. Table 2).

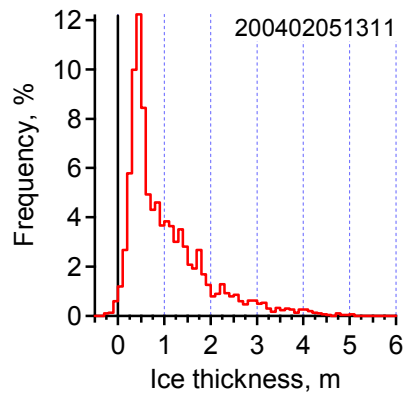
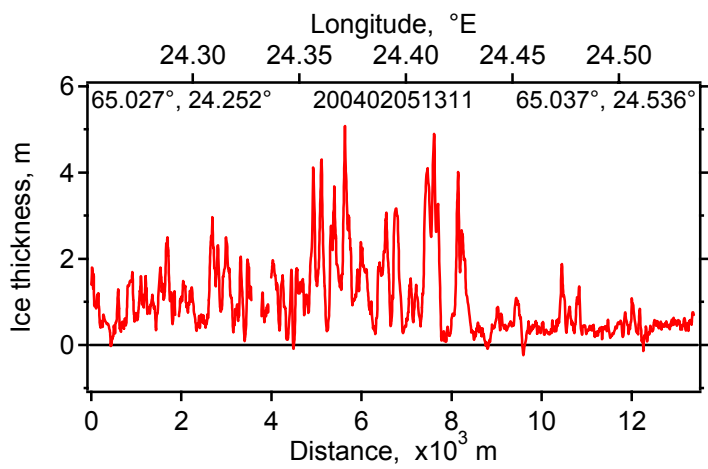
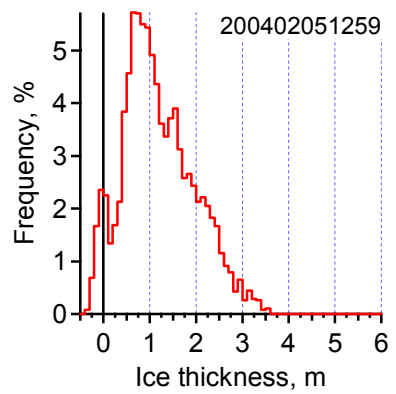
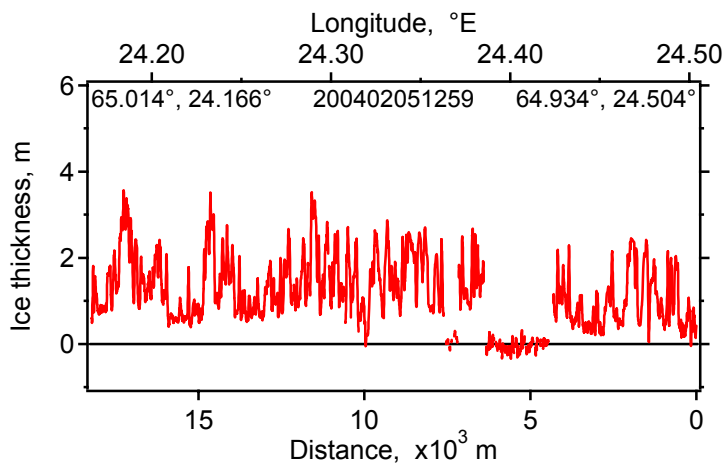
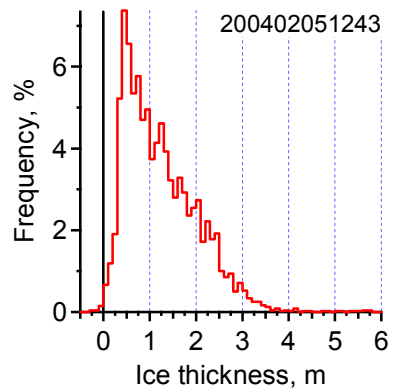
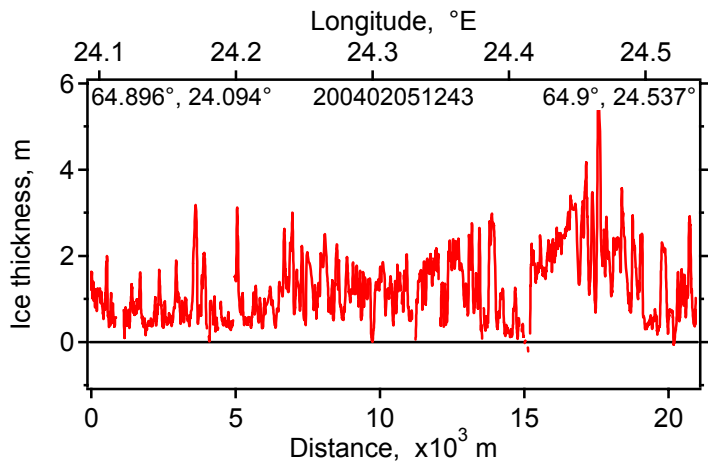
3.4 Profile plots

The following section presents ice thickness maps for each flight and the corresponding thickness profiles and histograms for each leg.

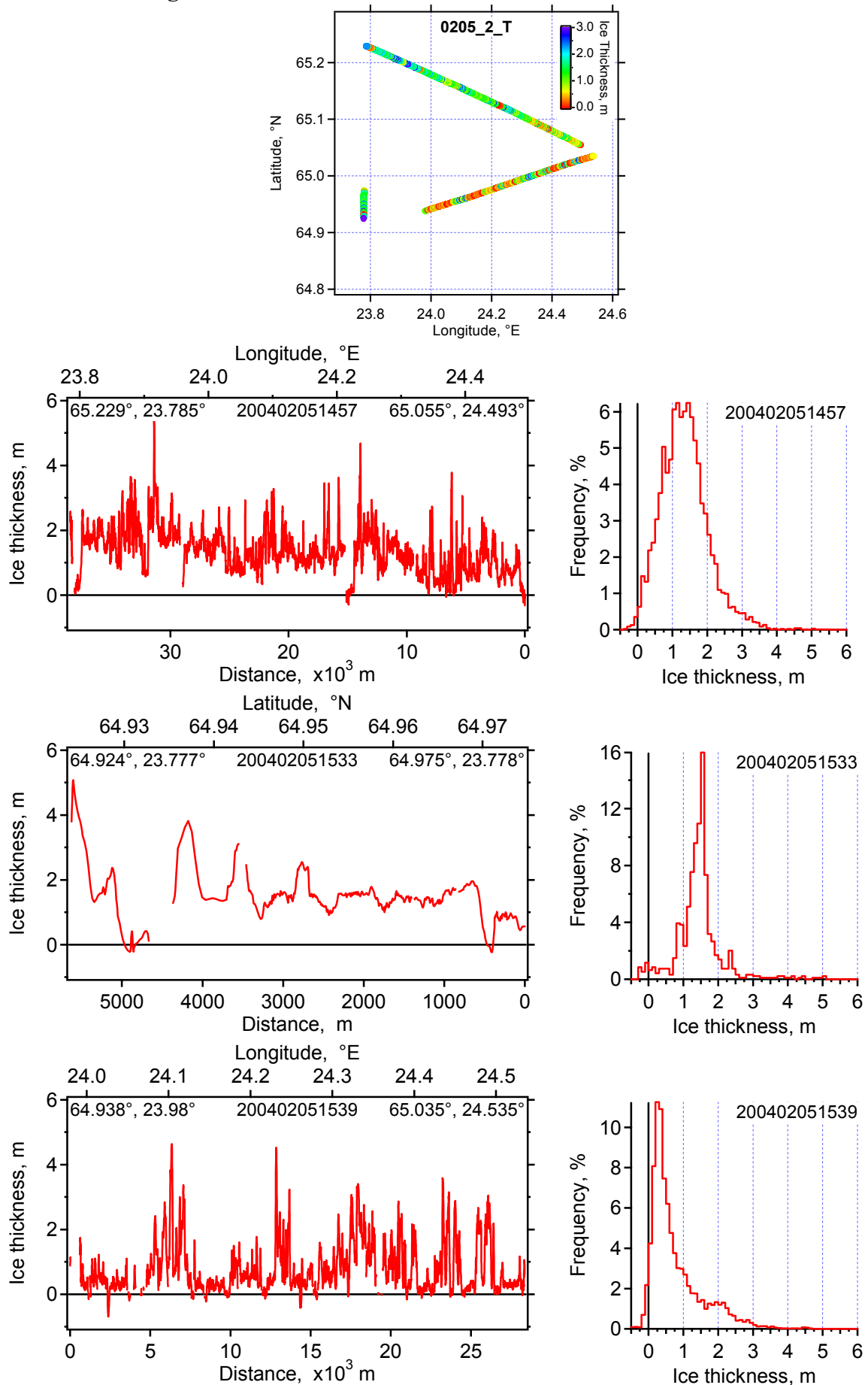
Plots are arranged chronologically for each flight, and presented from West to East (for the grid flights and the first and last leg of the triangle) or from South to North (for the second leg of the triangle). Positions of the end points as well as the distance from the beginning of each profile are also shown.

05.2.2004 Grid

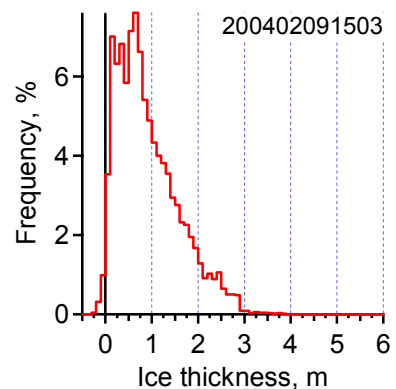
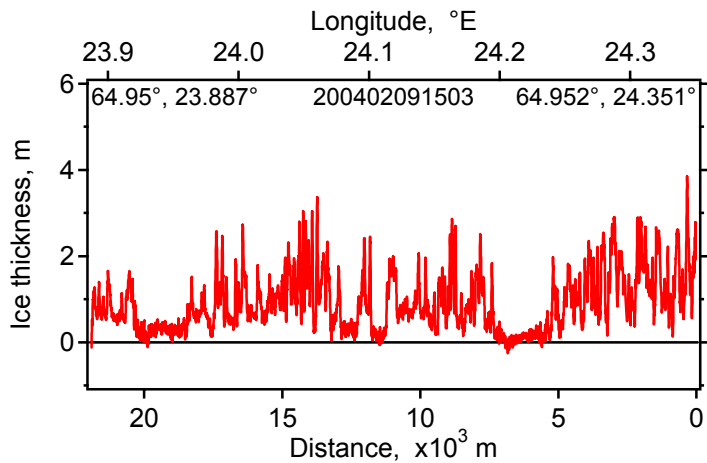
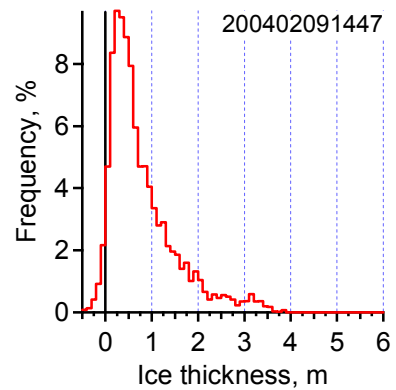
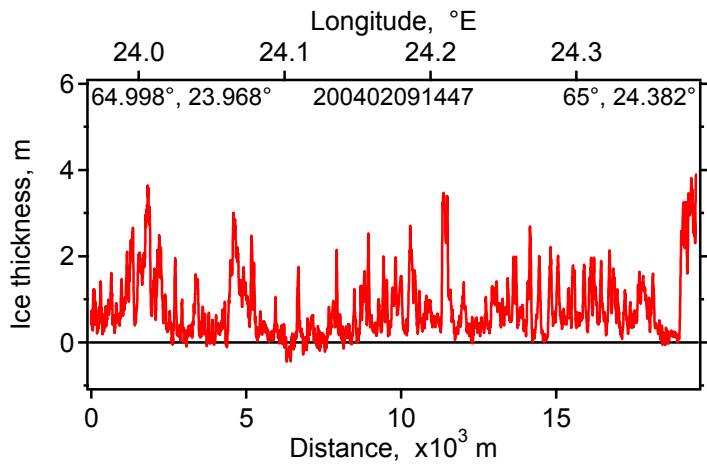
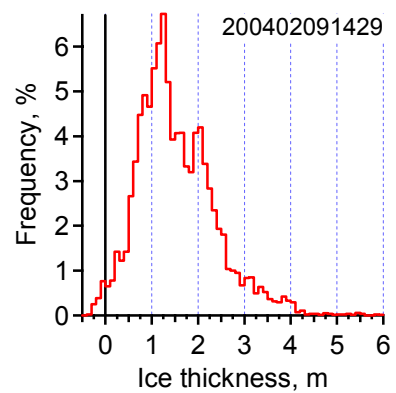
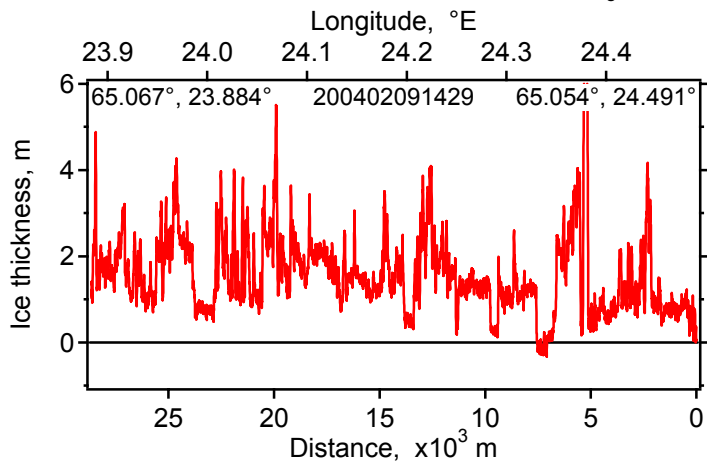
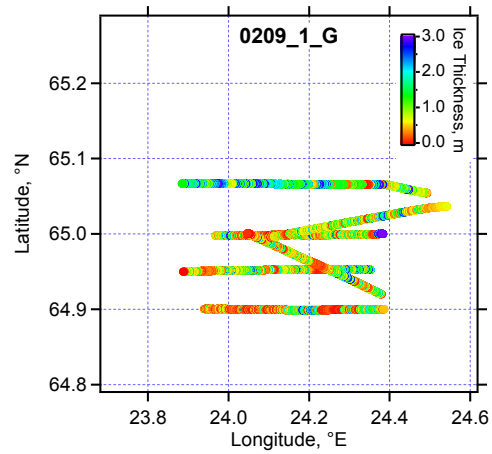


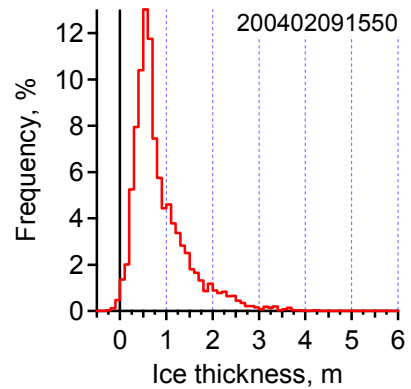
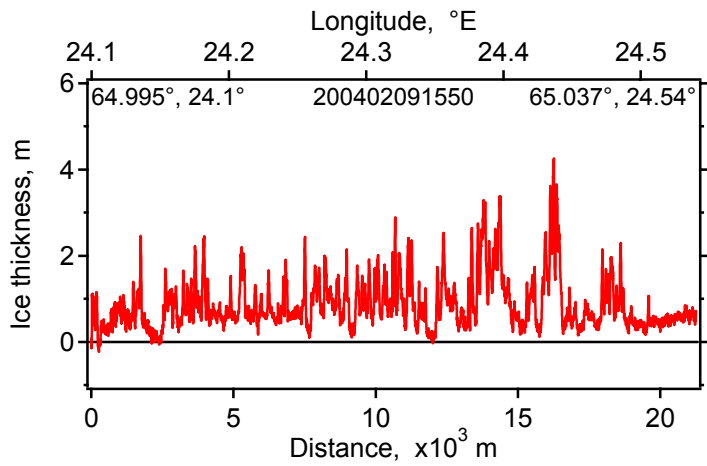
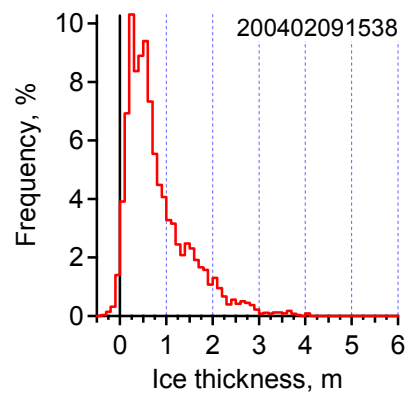
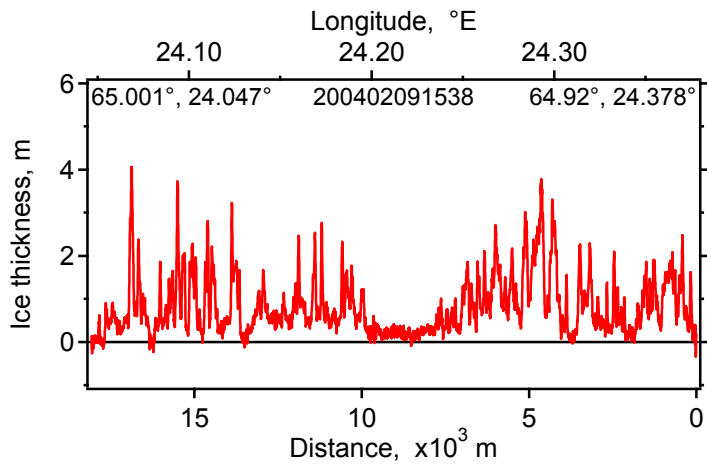
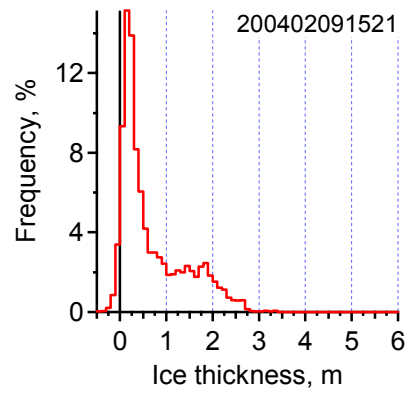
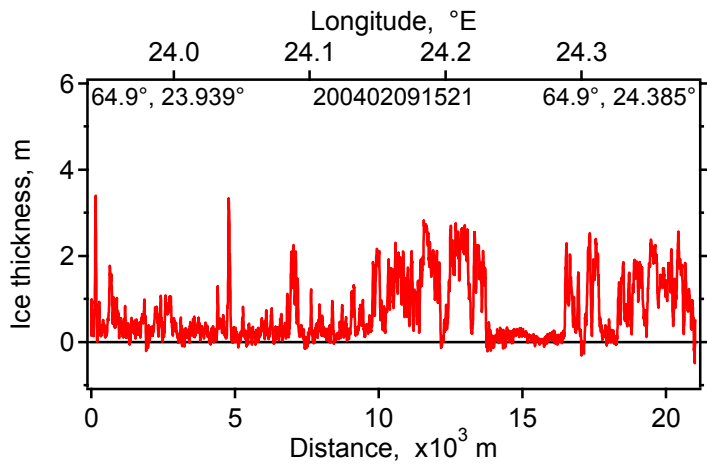


05.2.2004 Triangle

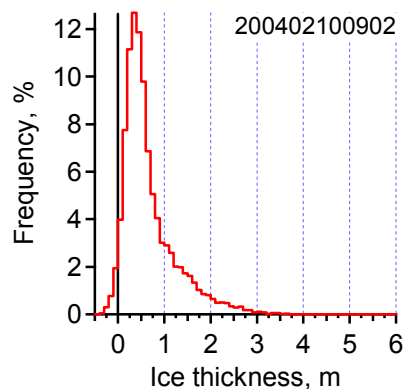
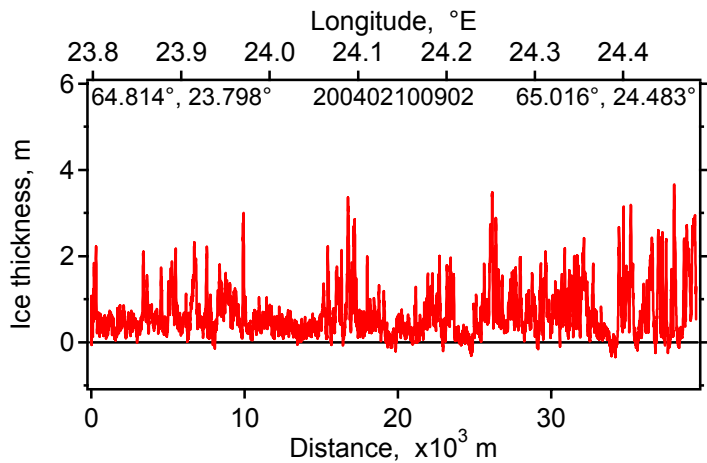
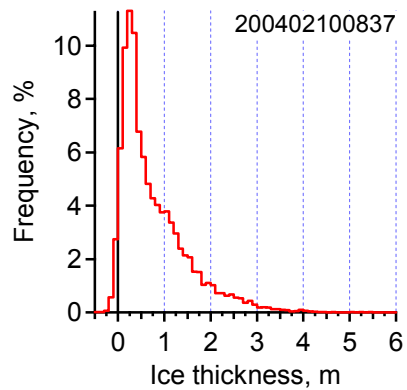
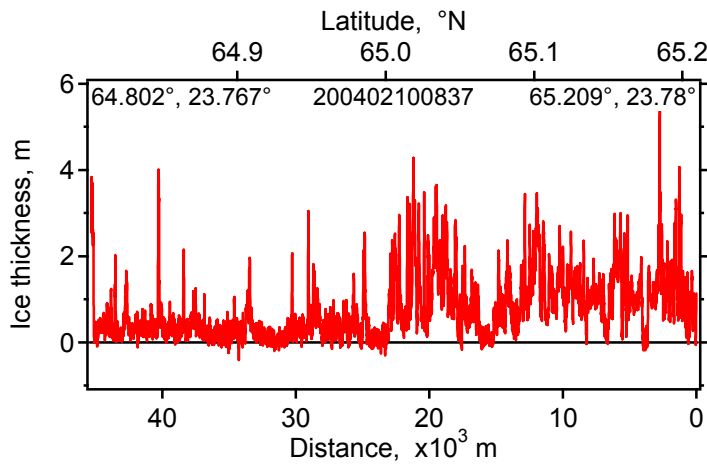
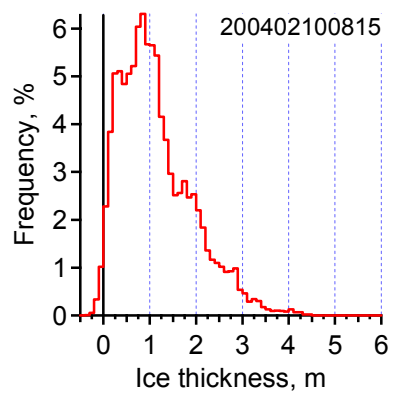
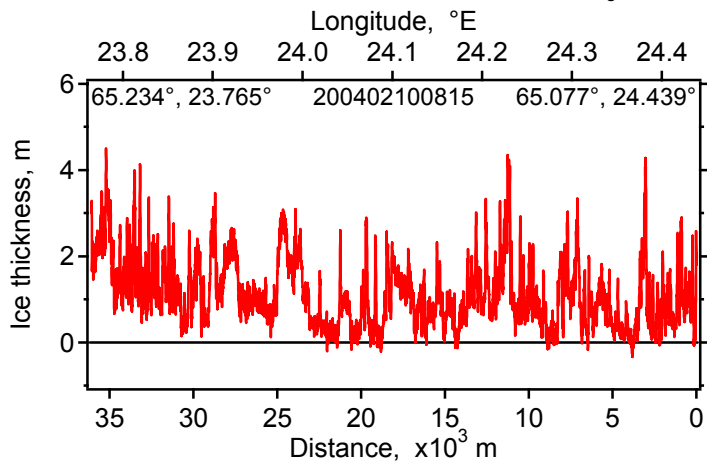
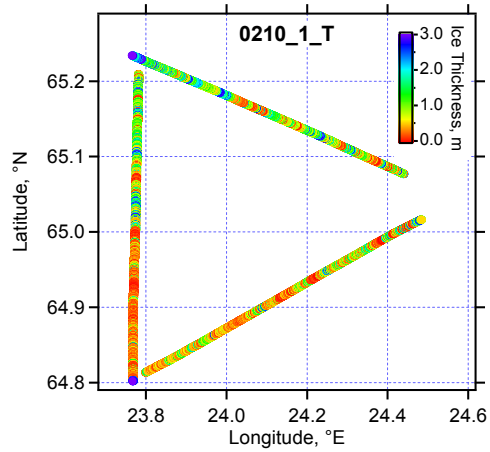


09.2.2004 Grid

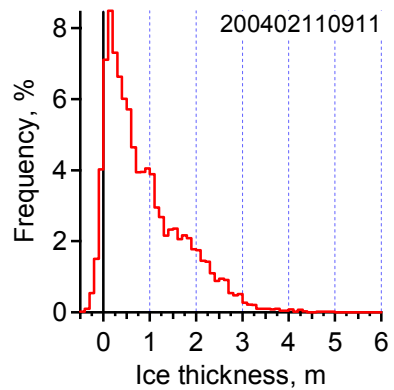
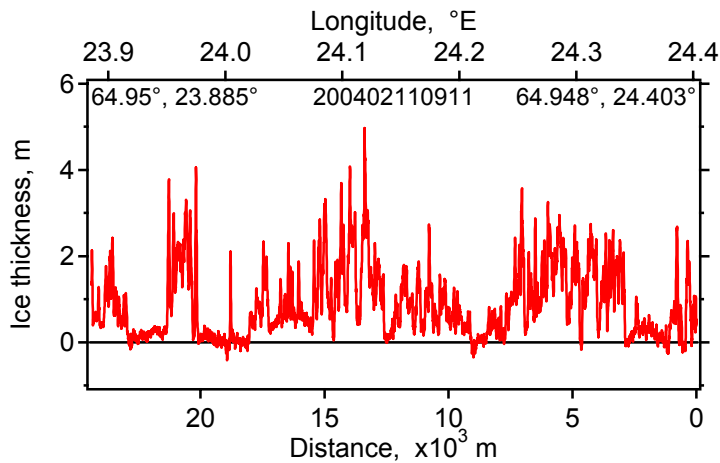
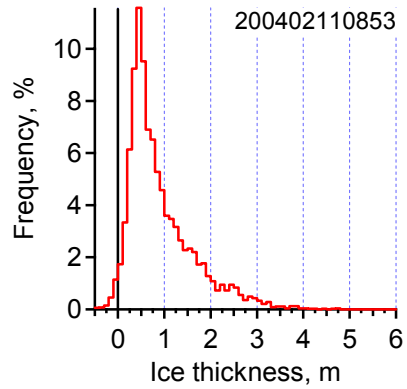
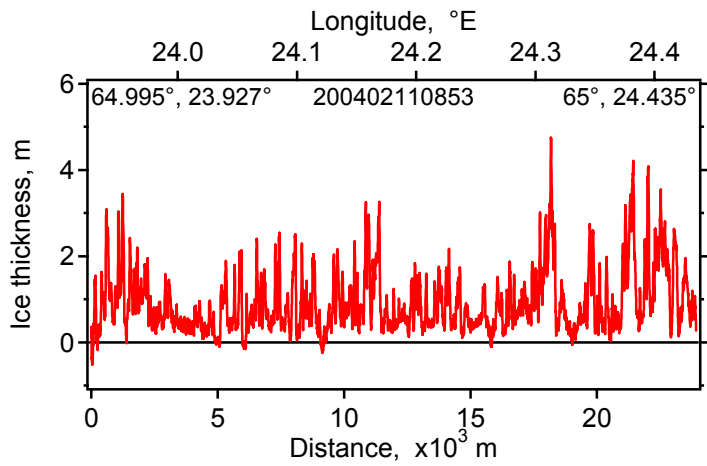
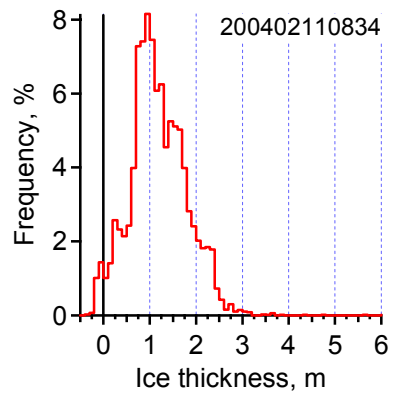
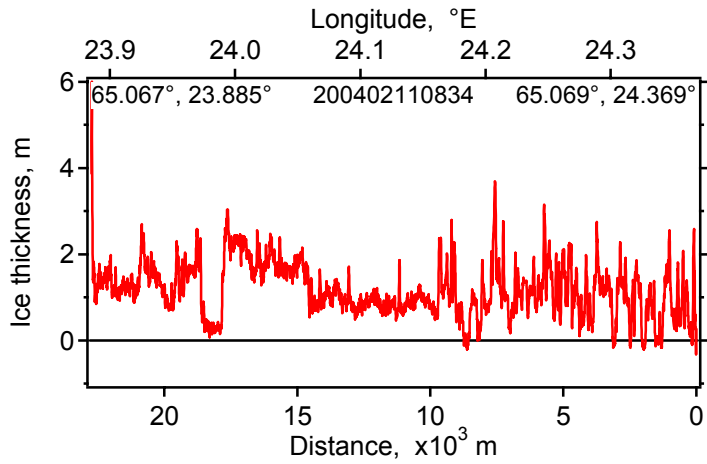
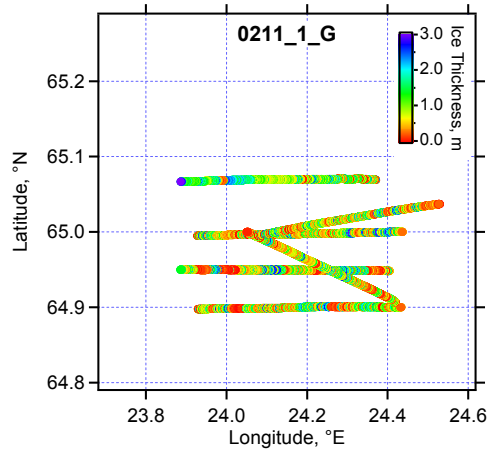


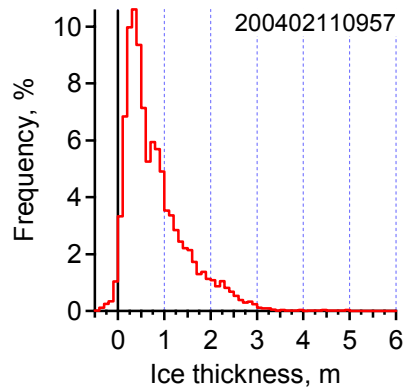
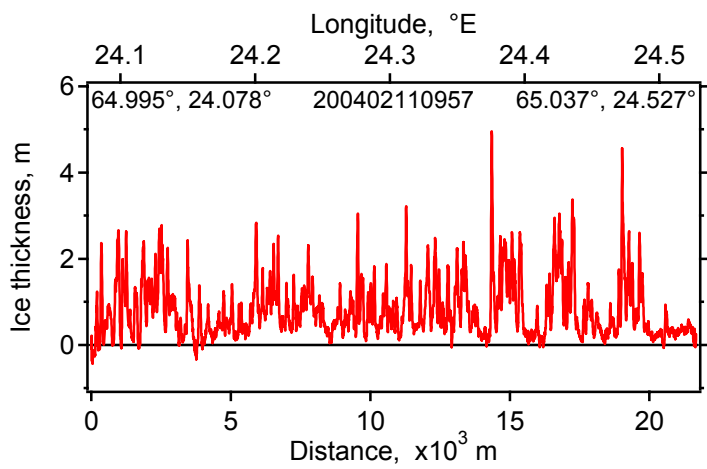
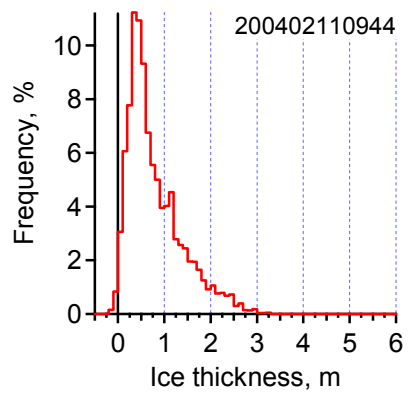
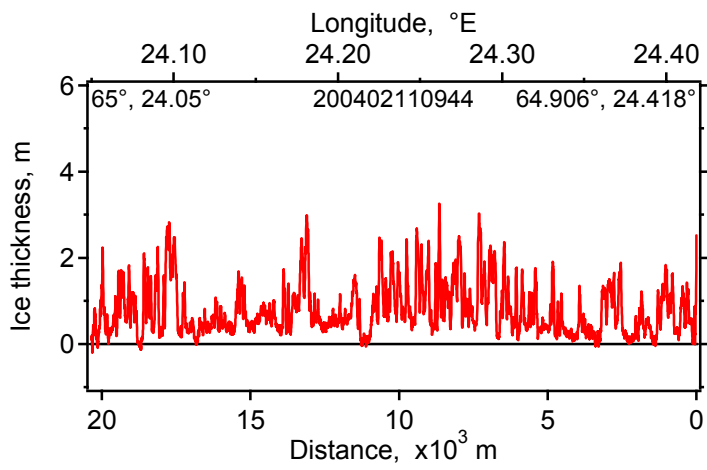
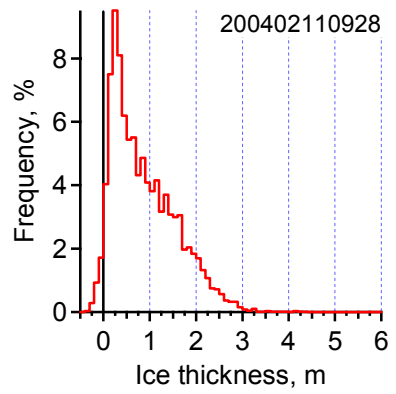
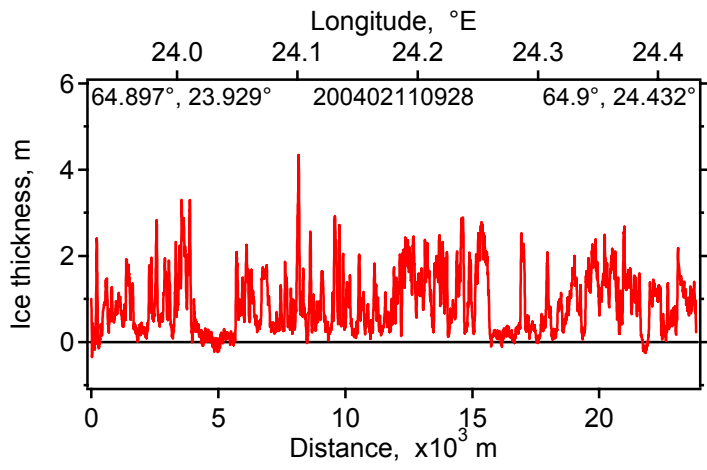


10.2.2004 Triangle

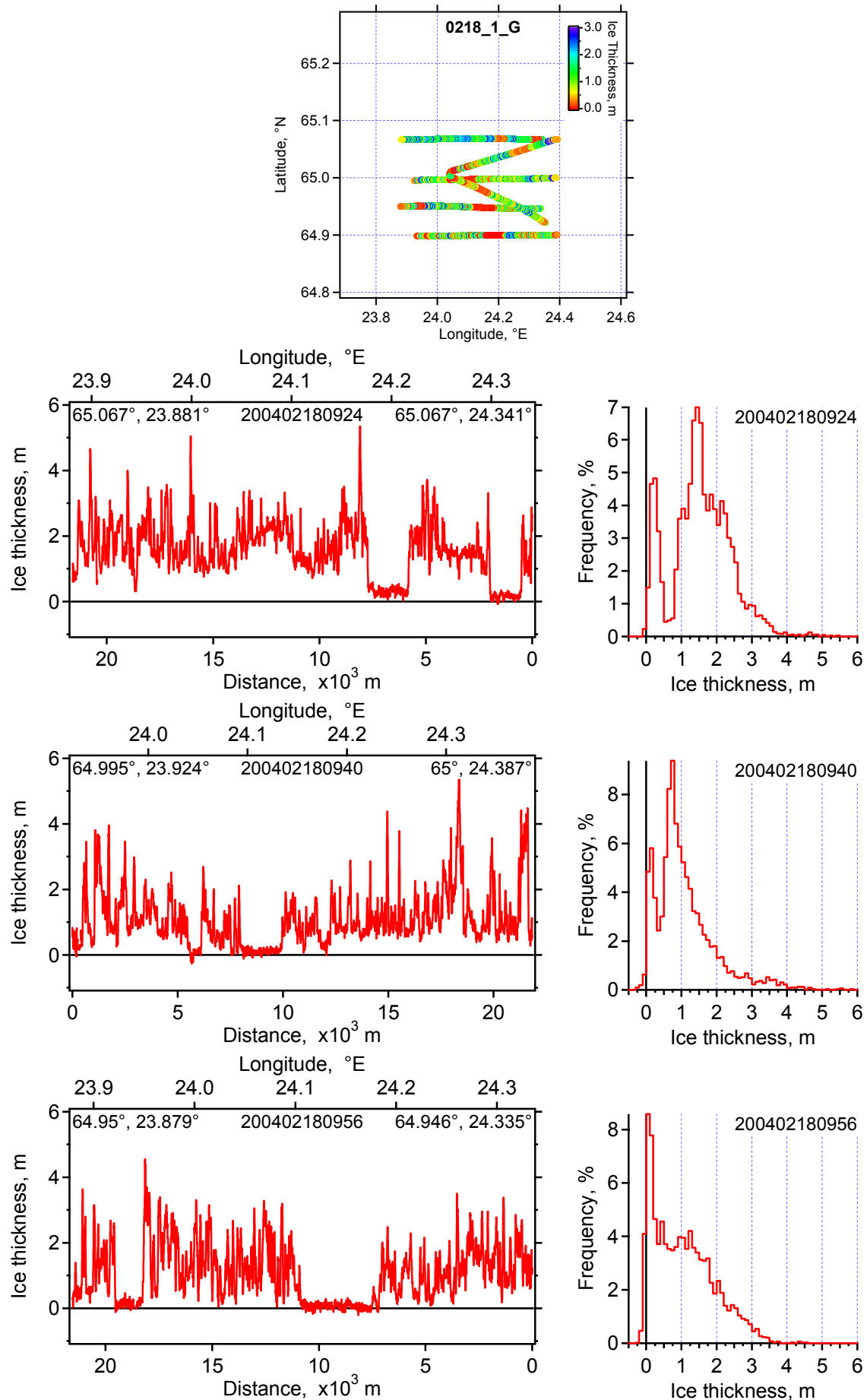


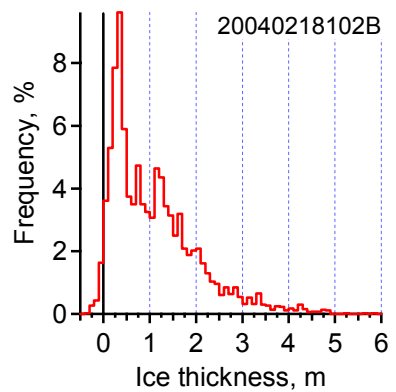
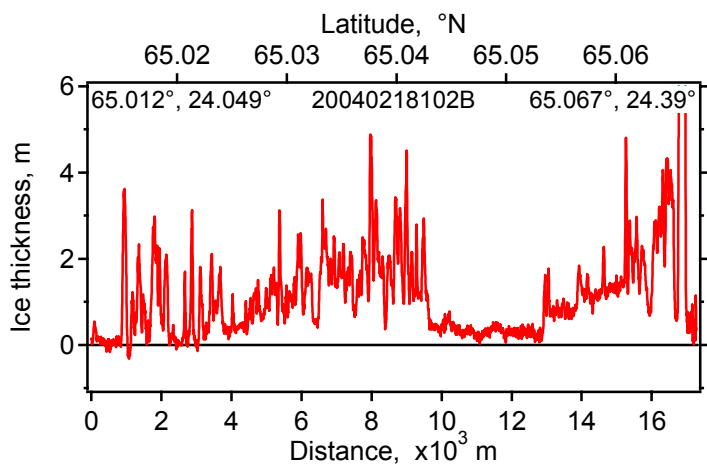
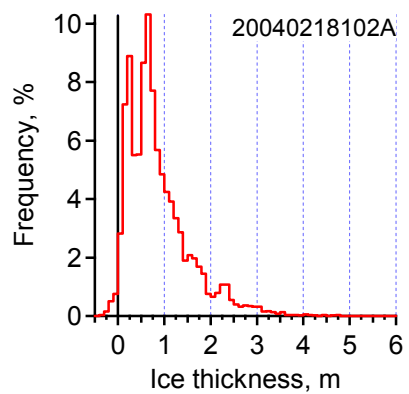
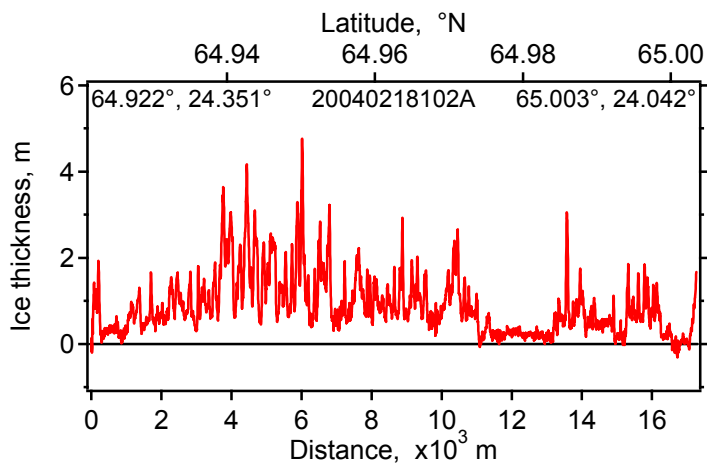
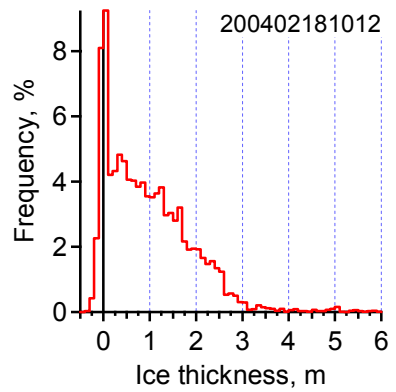
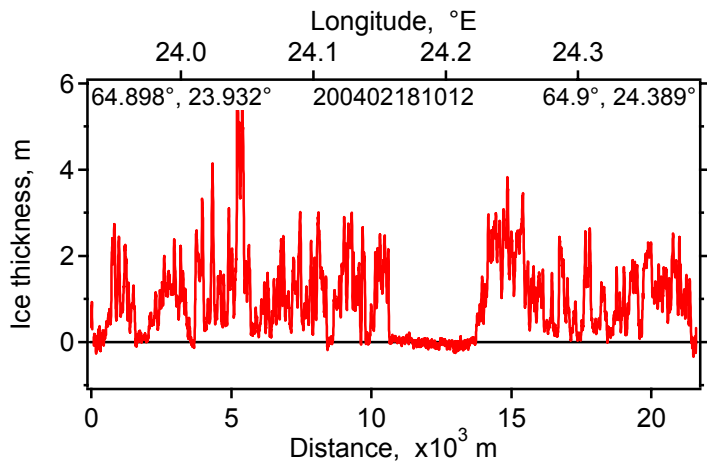
11.2.2004 Grid



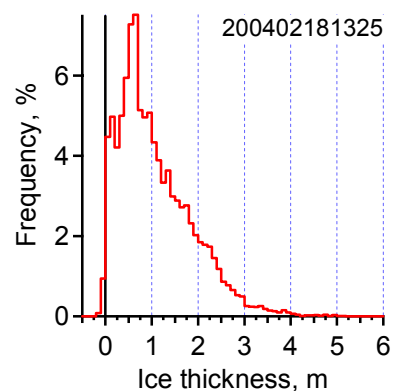
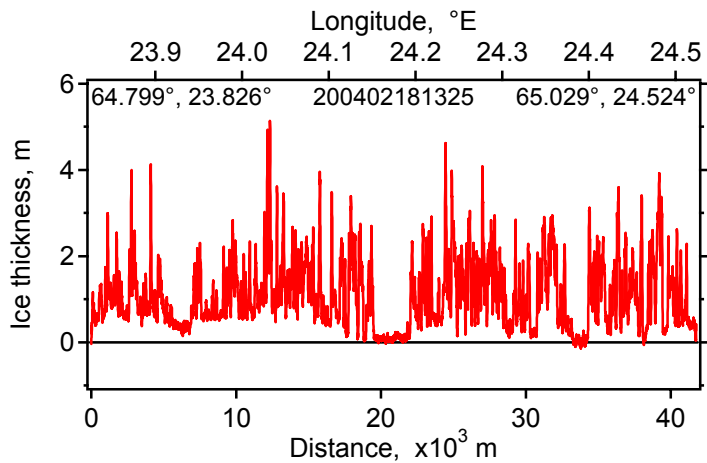
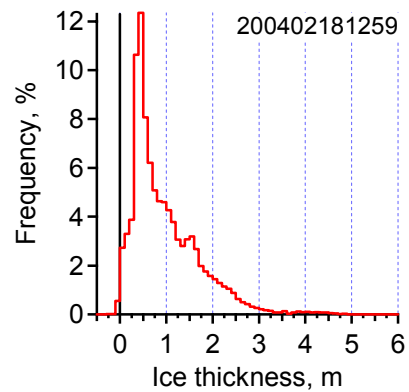
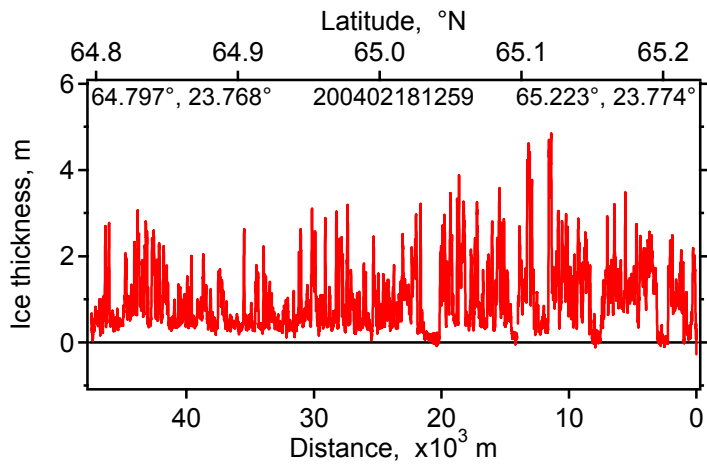
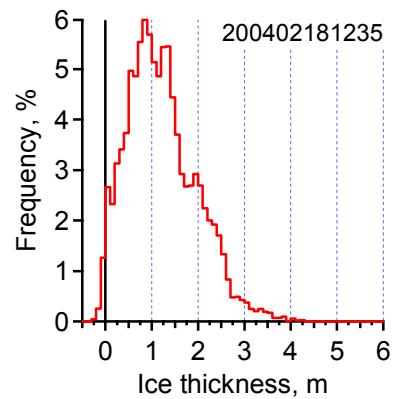
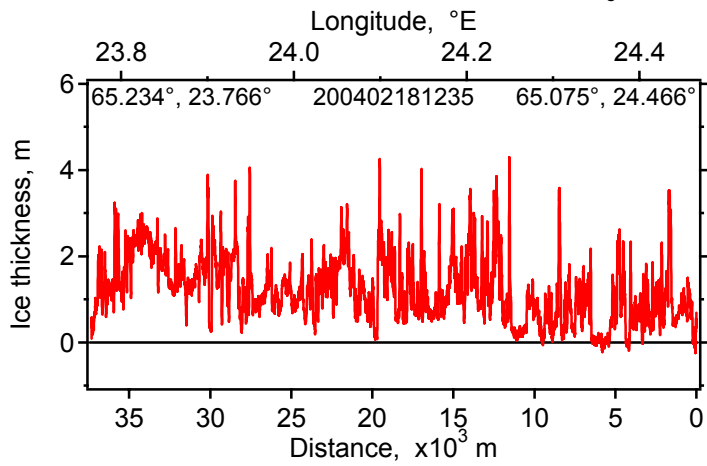
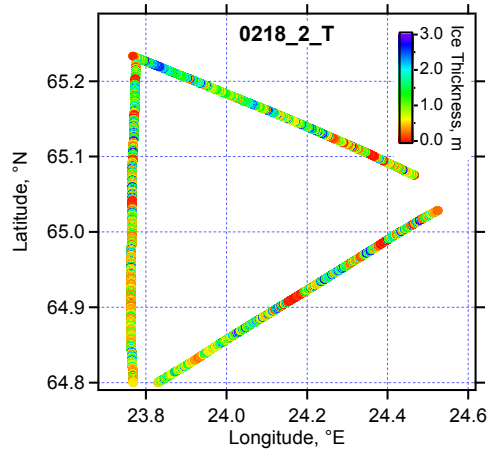


18.2.2004 Grid

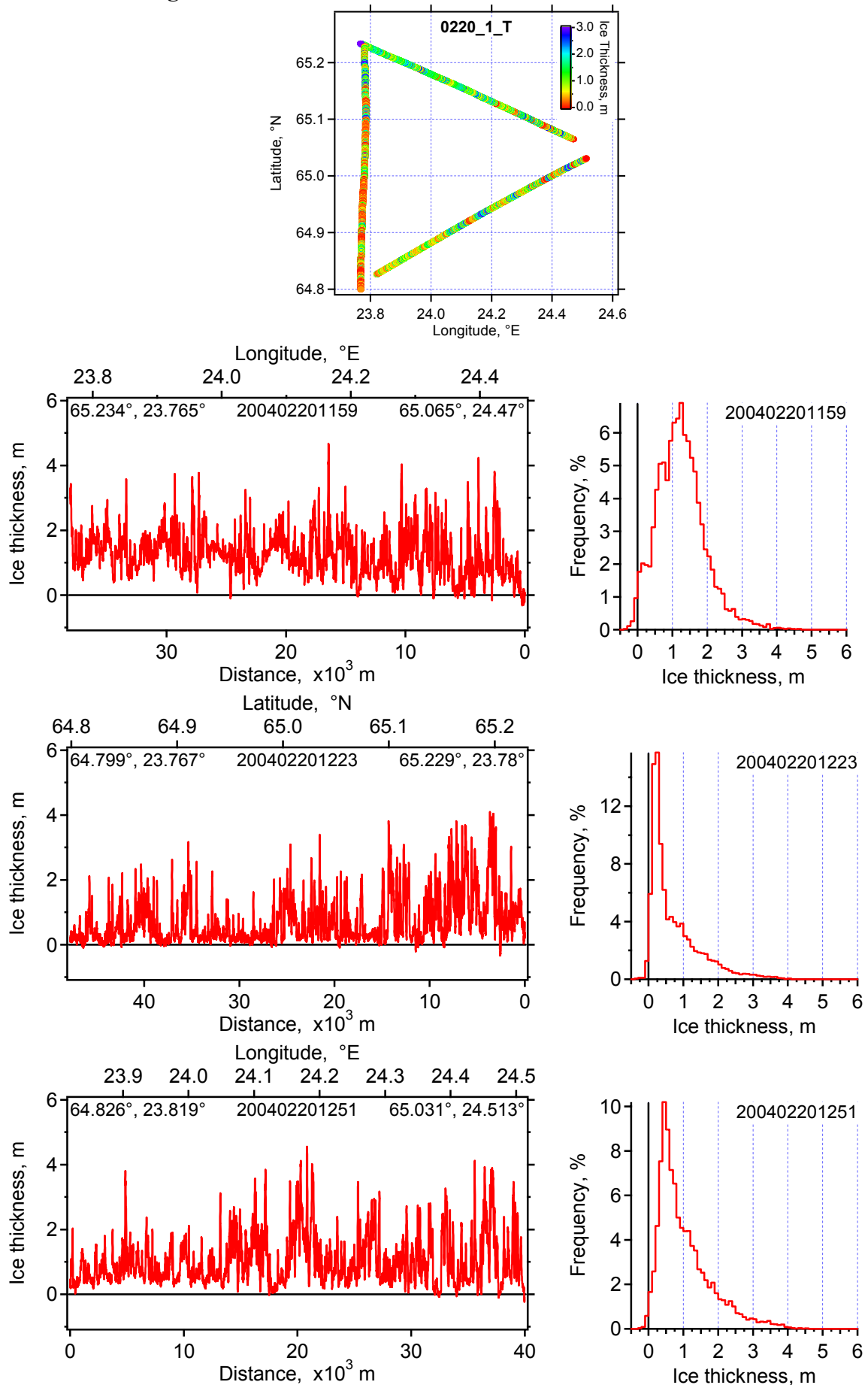




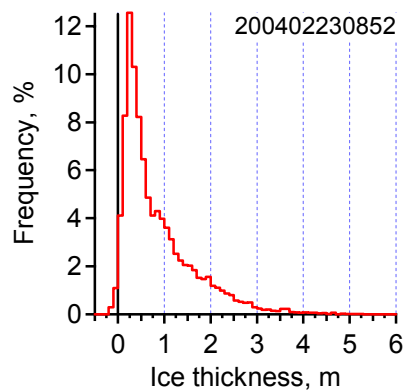
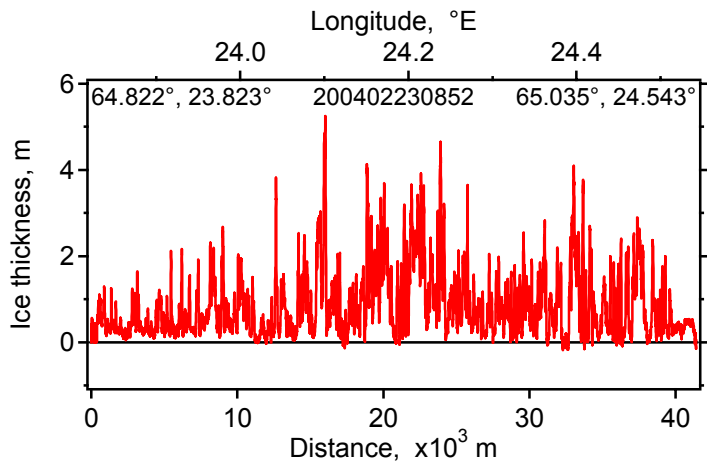
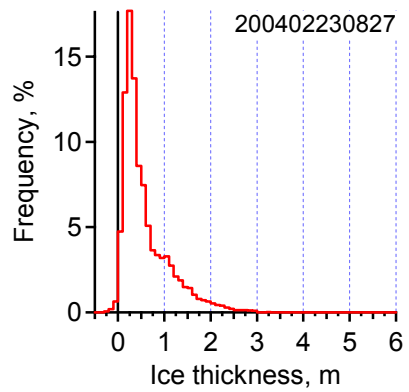
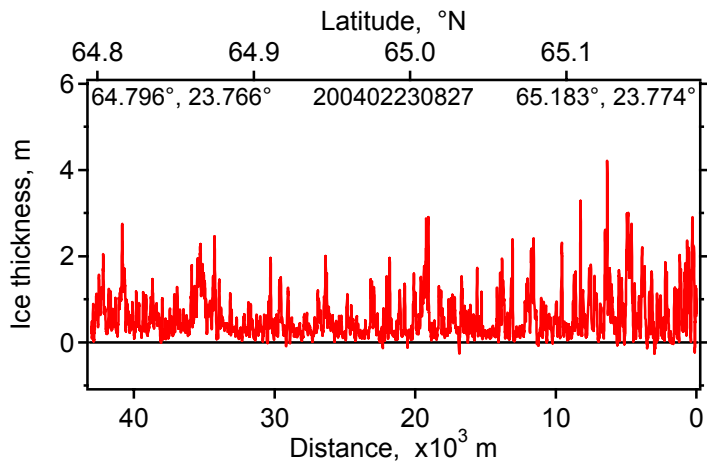
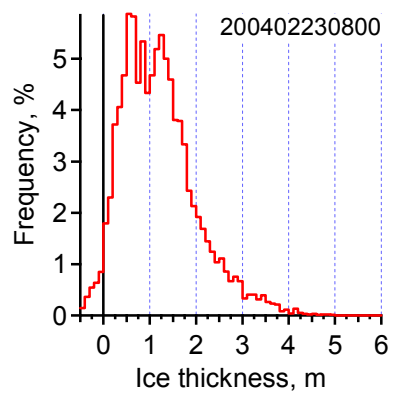
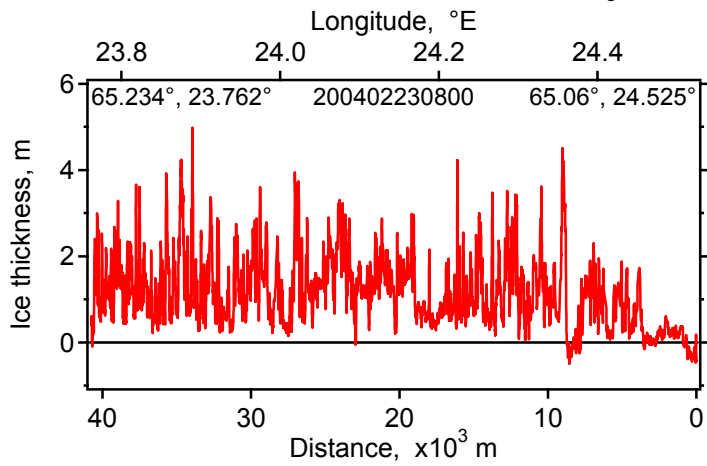
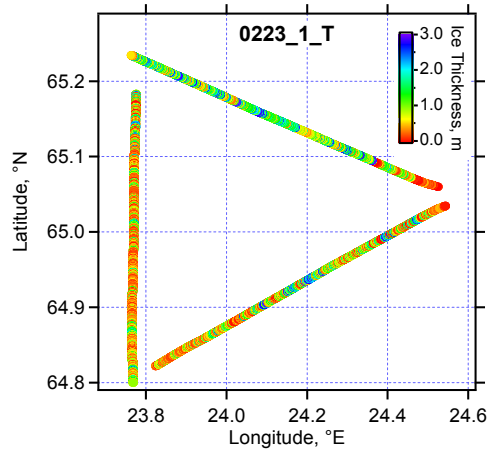
18.2.2004 Triangle



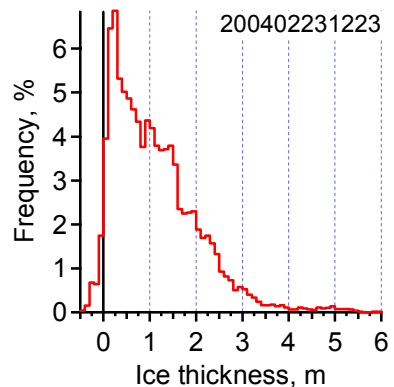
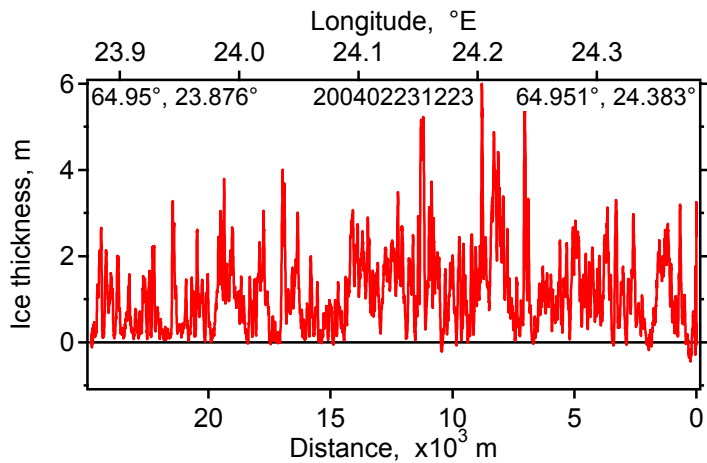
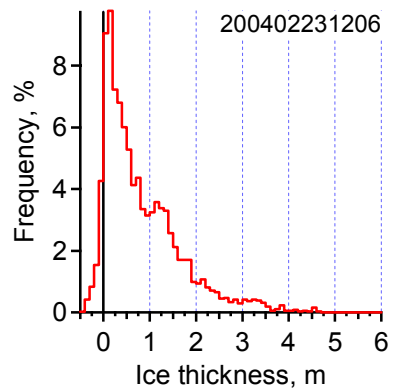
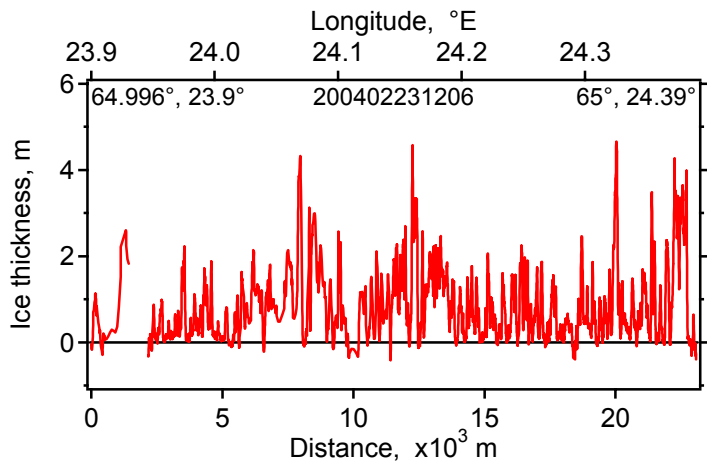
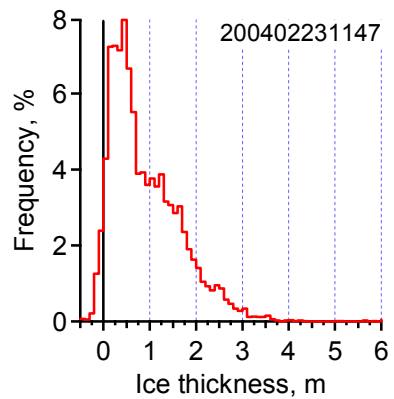
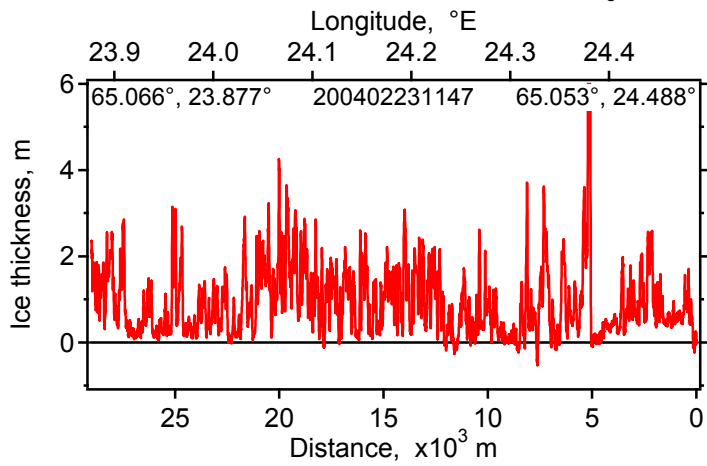
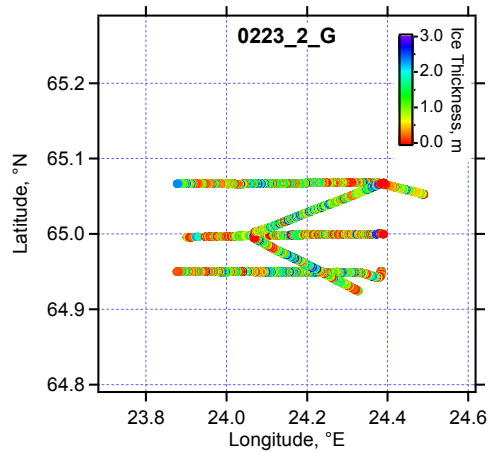
20.2.2004 Triangle

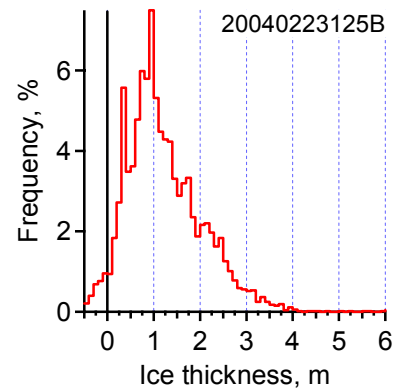
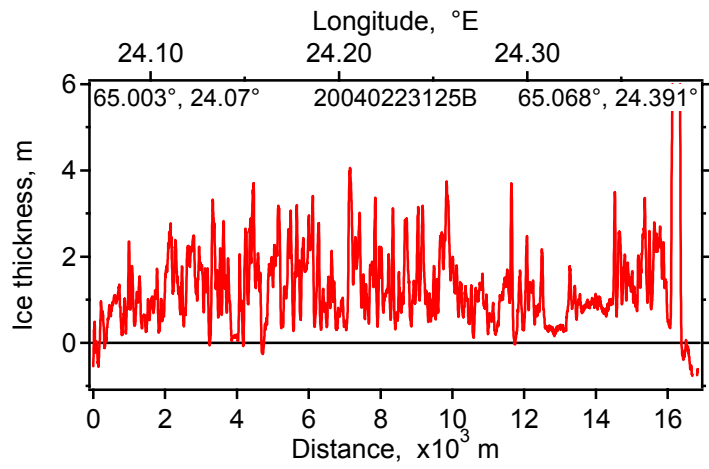
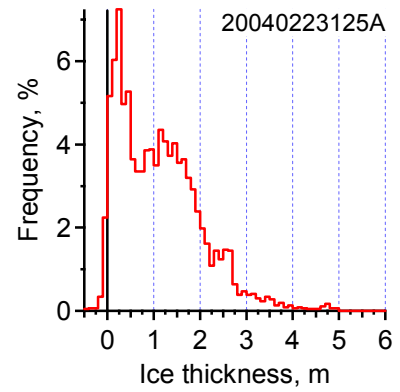
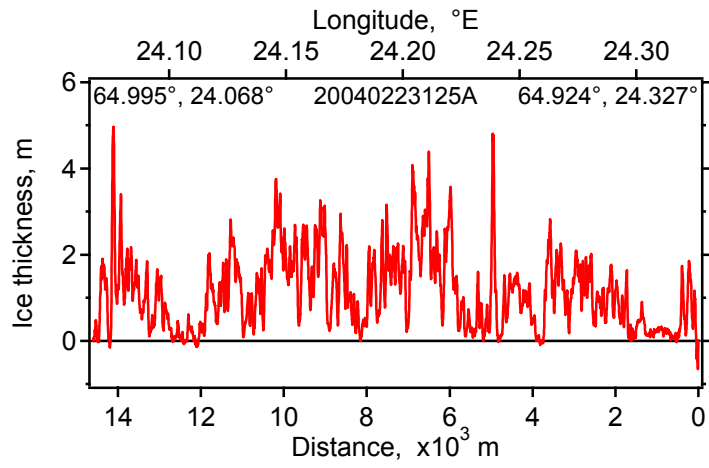


23.2.2004 Triangle

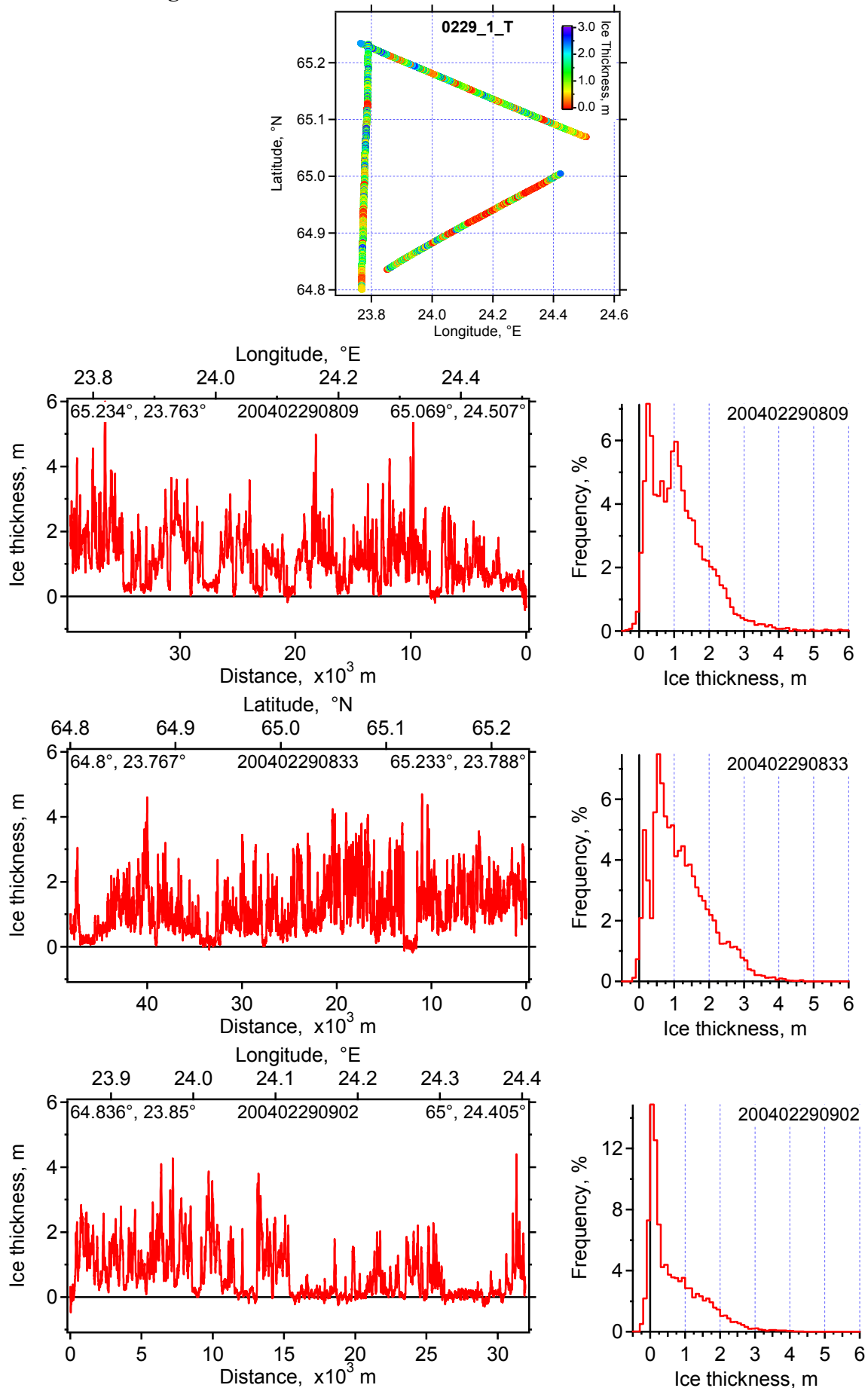


23.2.2004 Grid

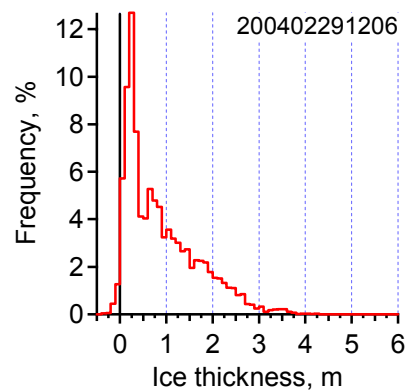
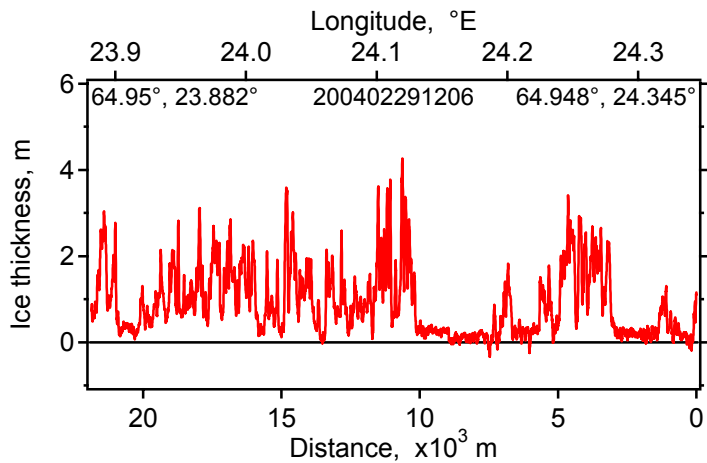
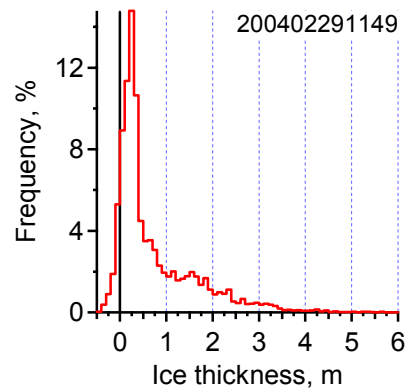
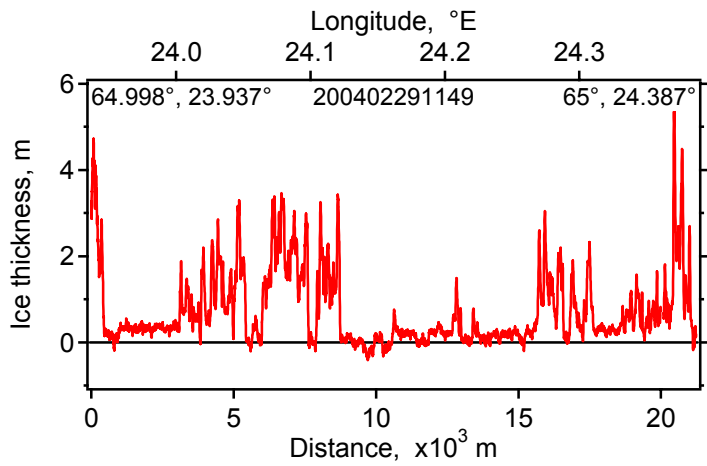
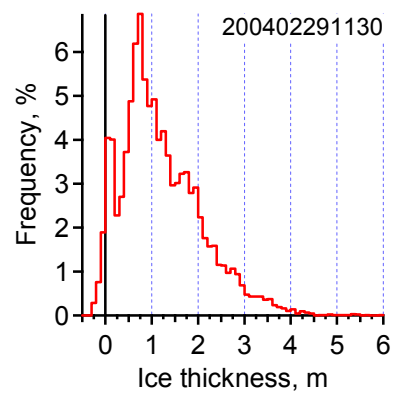
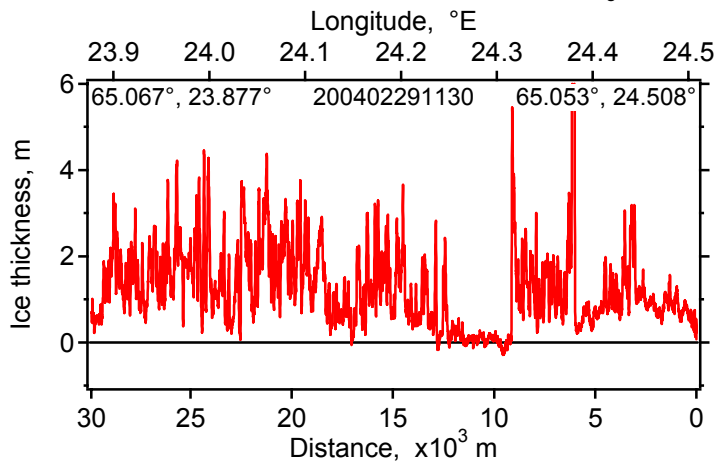
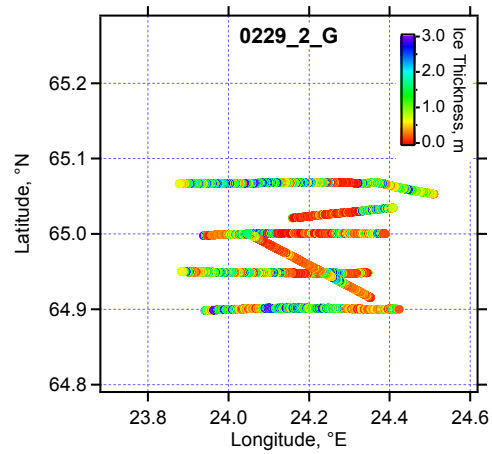


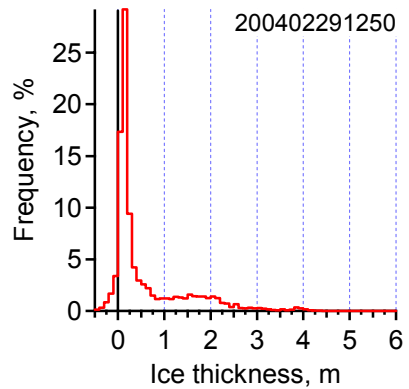
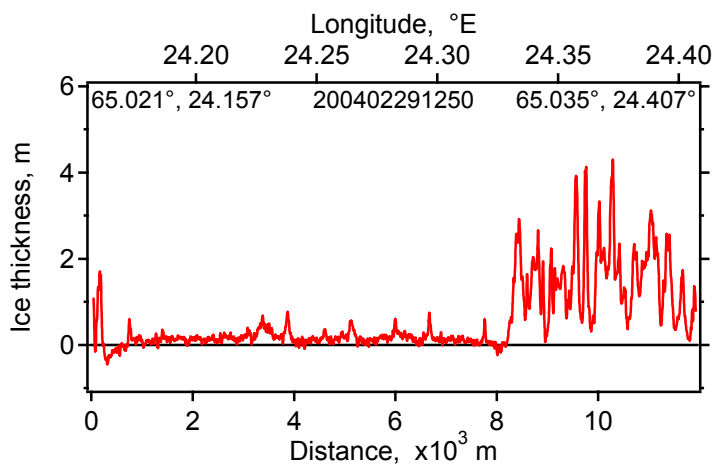
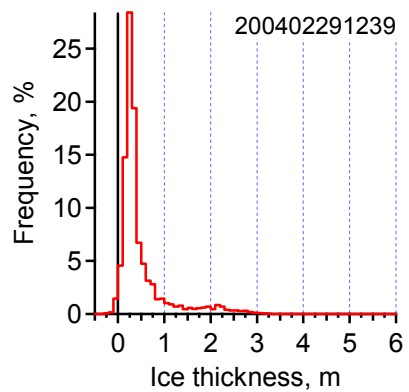
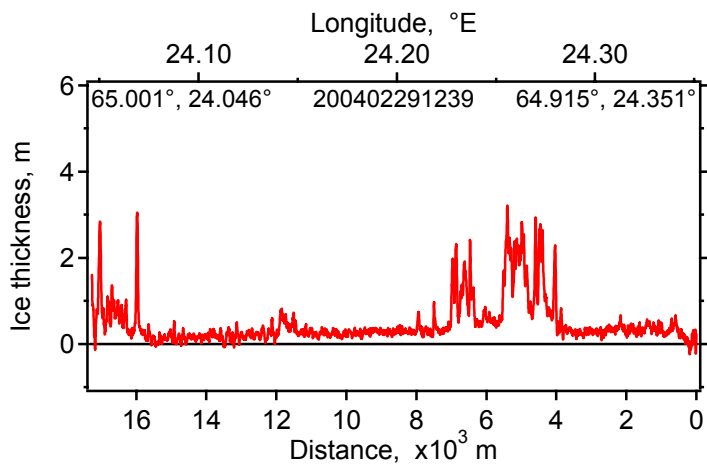
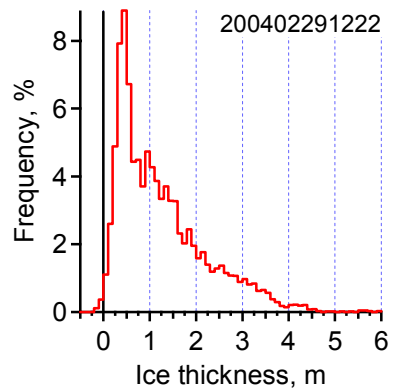
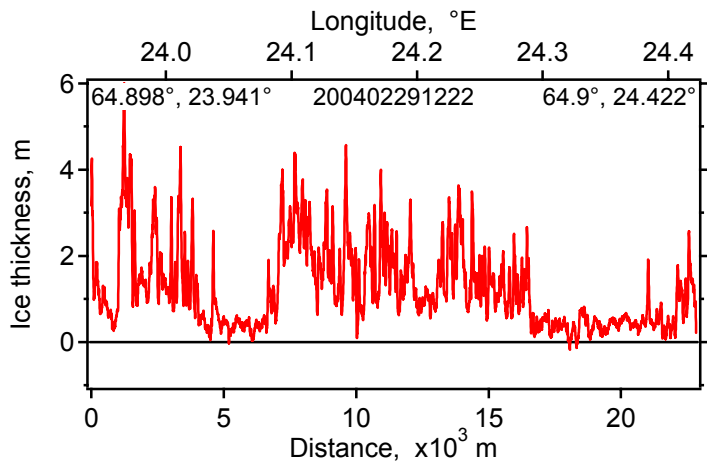


29.2.2004 Triangle

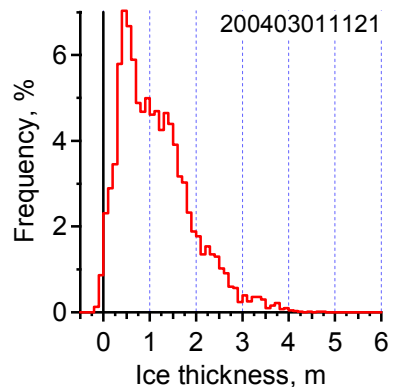
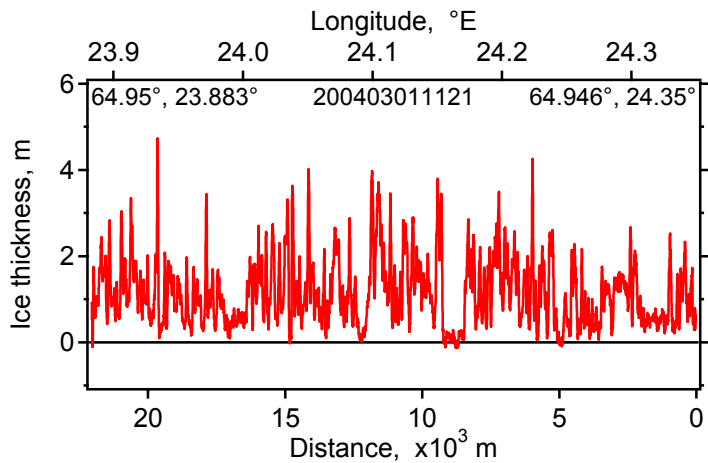
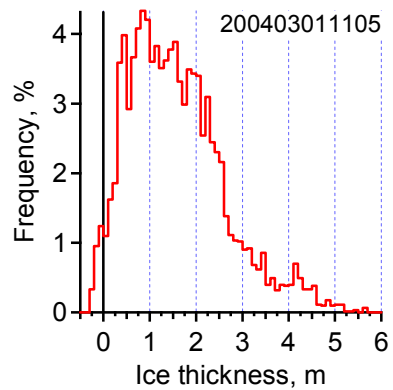
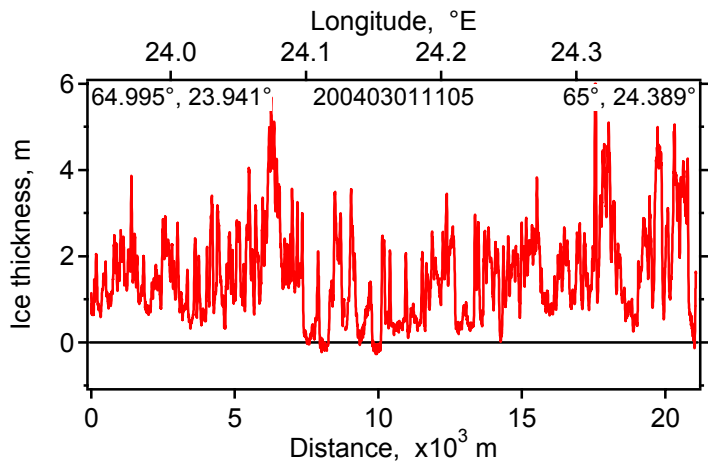
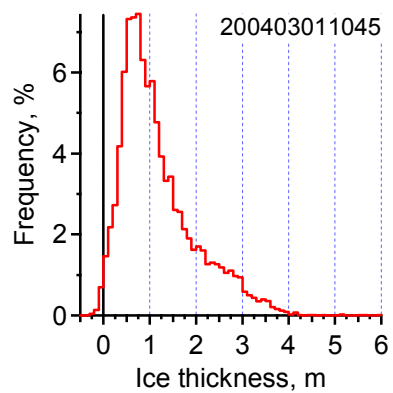
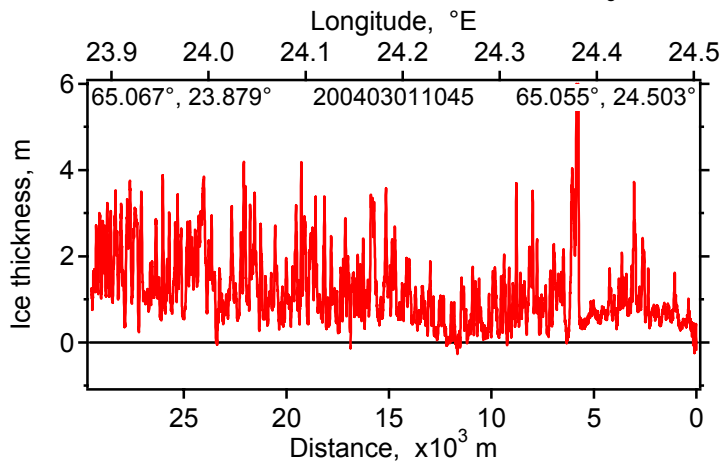
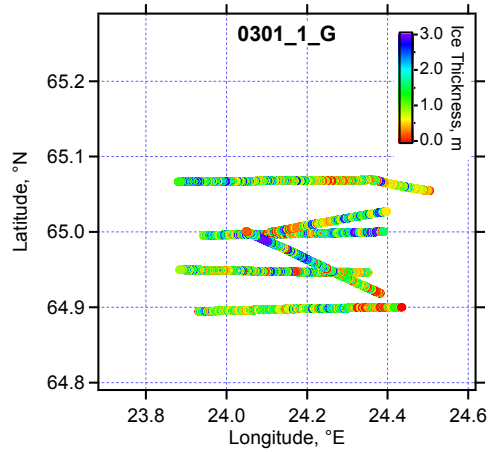


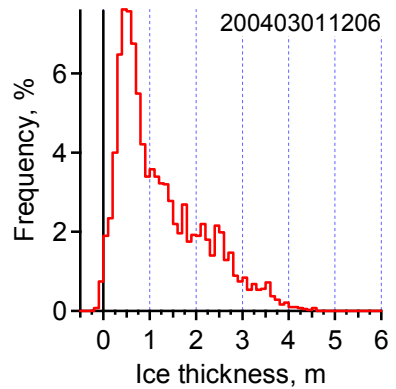
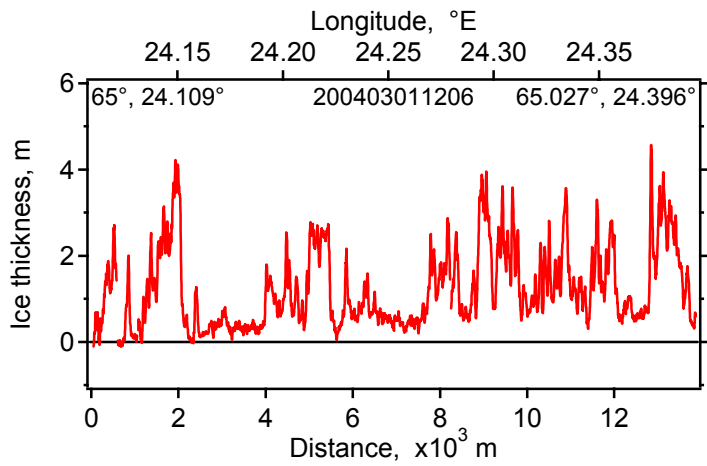
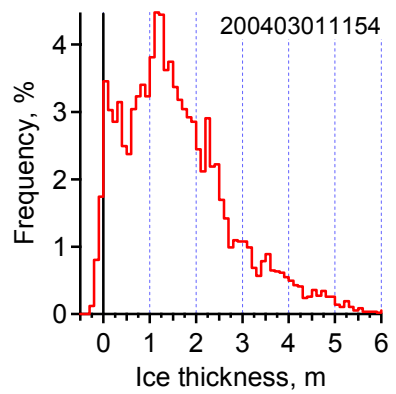
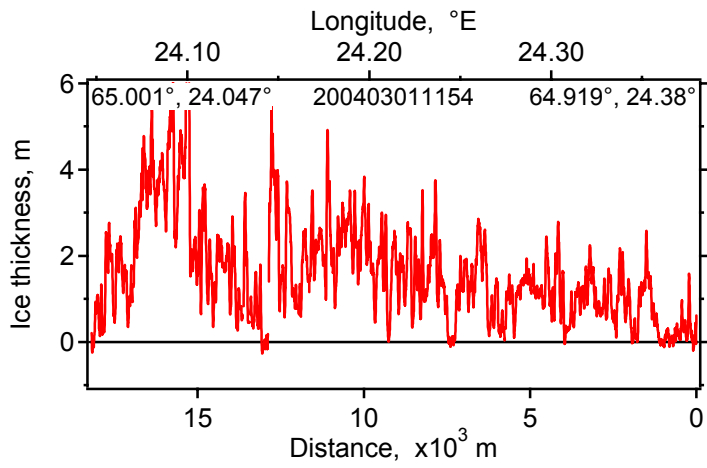
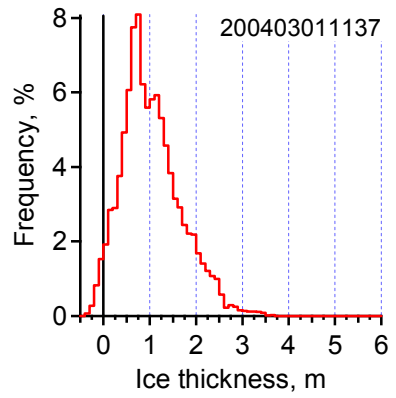
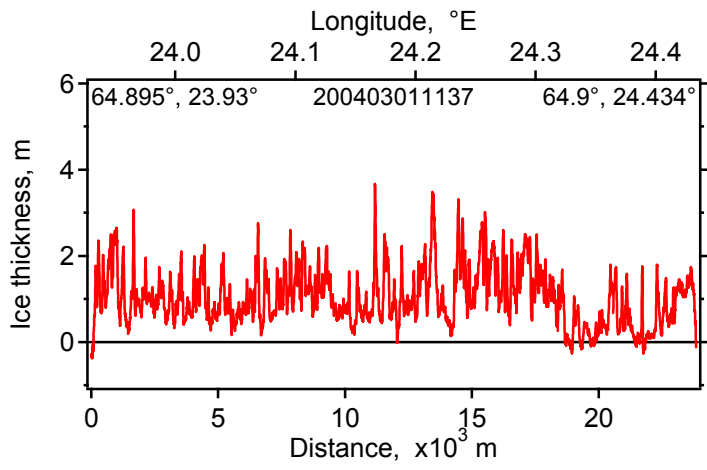
29.2.2004 Grid



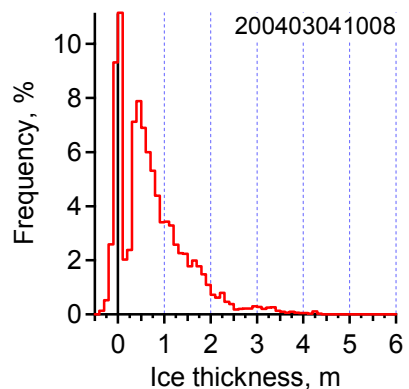
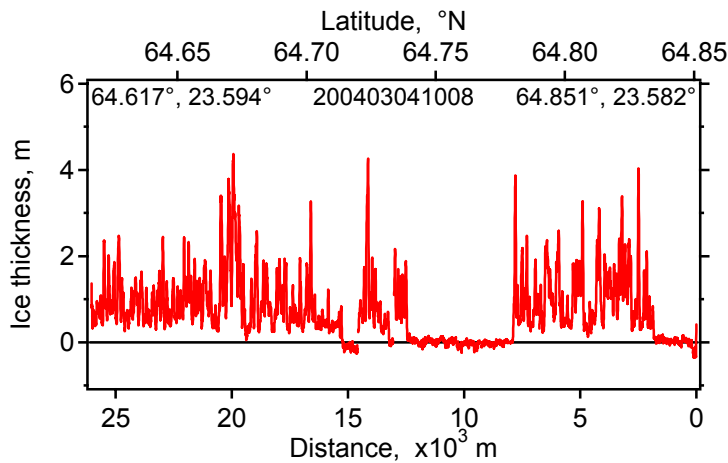
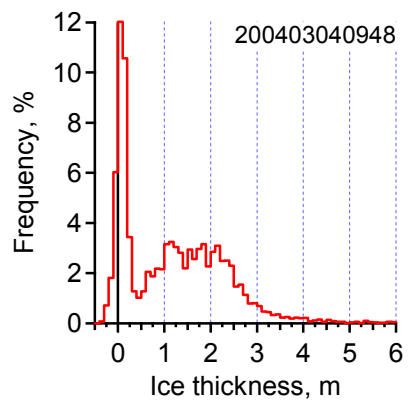
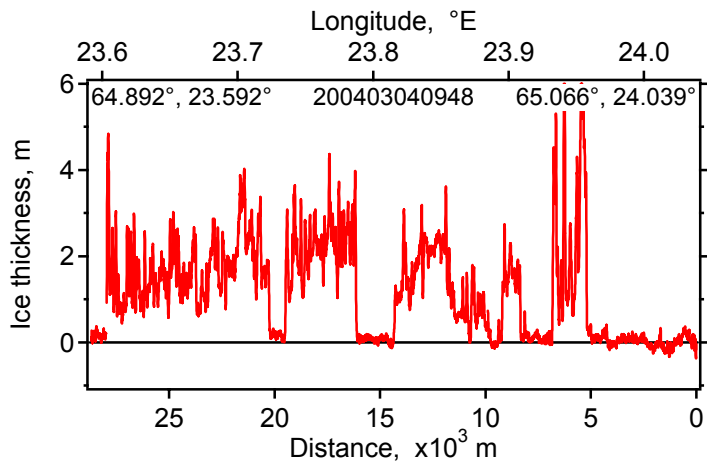
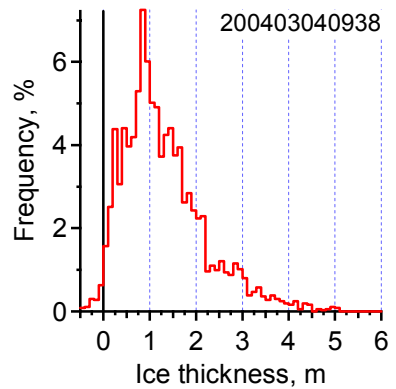
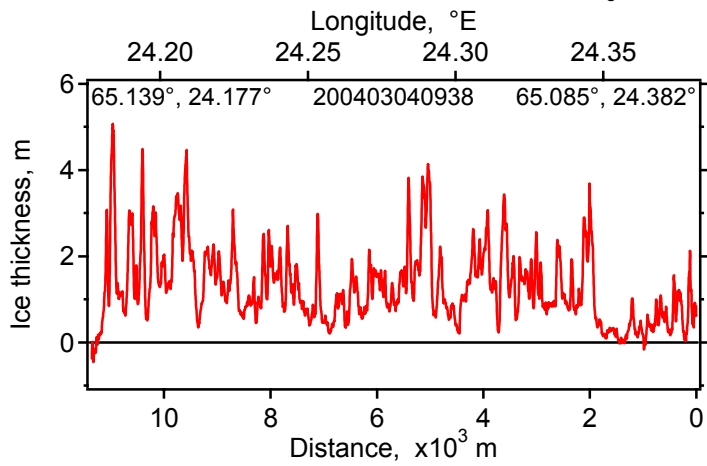
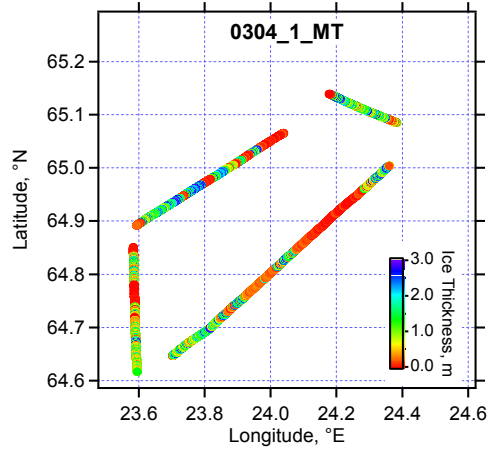


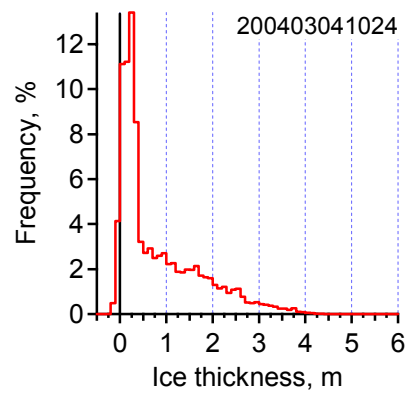
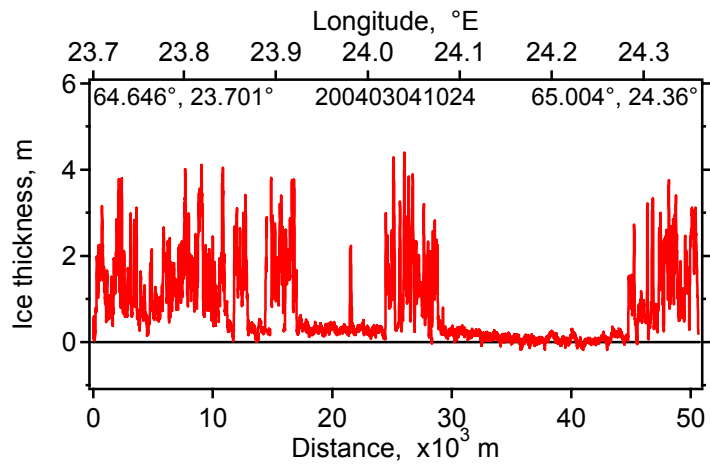
01.3.2004 Grid



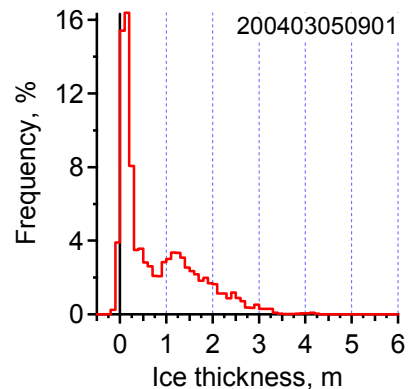
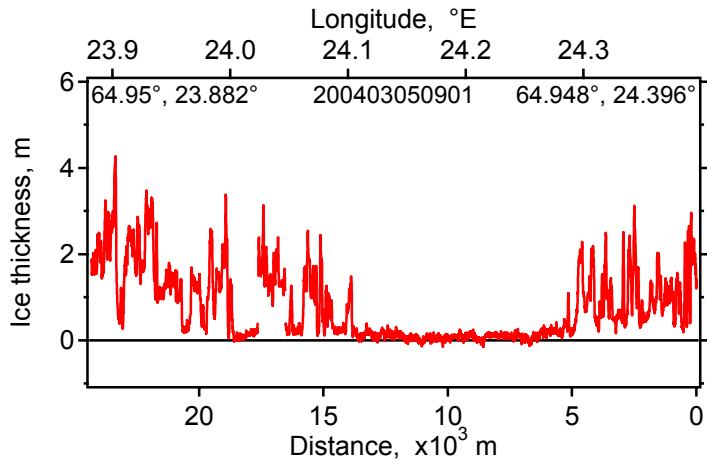
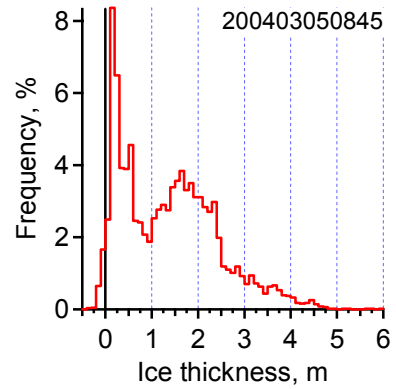
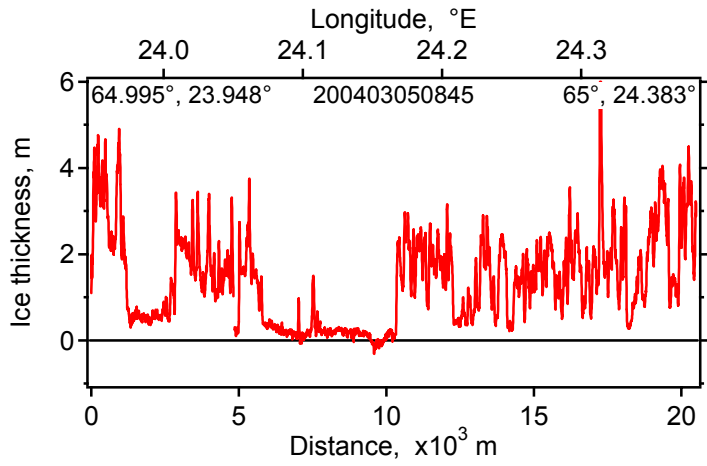
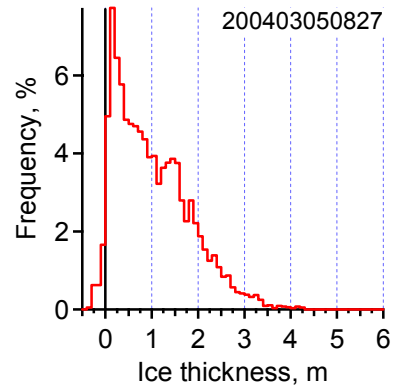
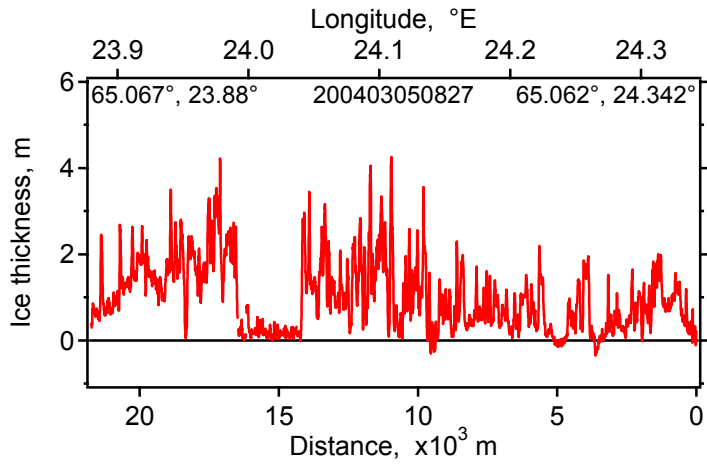
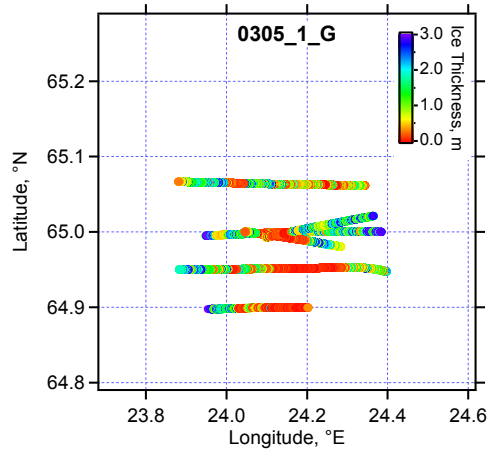


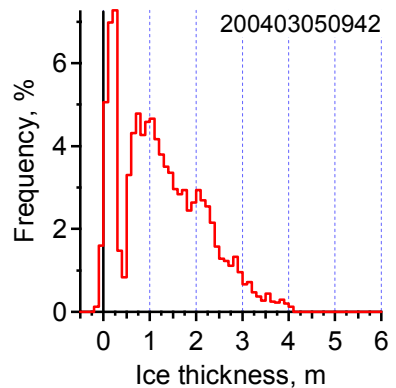
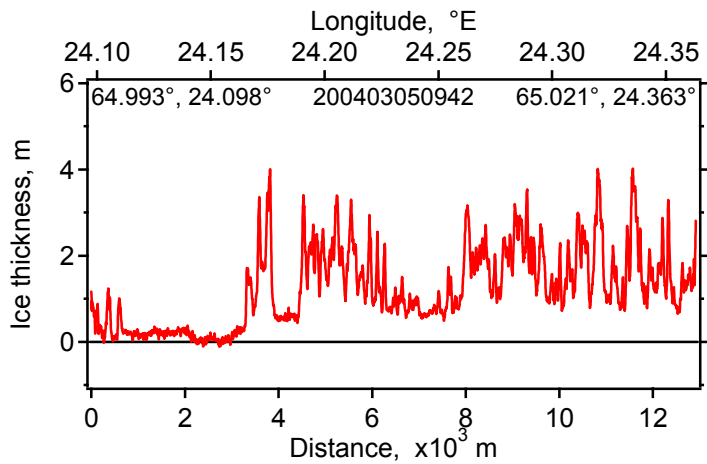
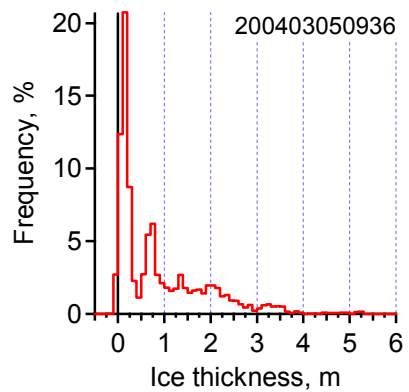
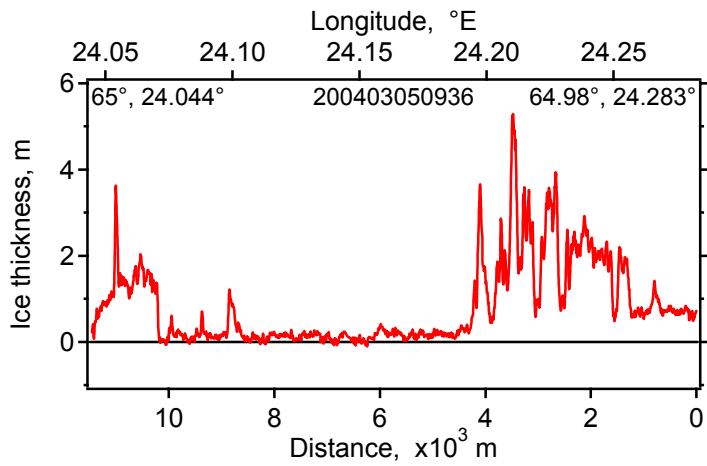
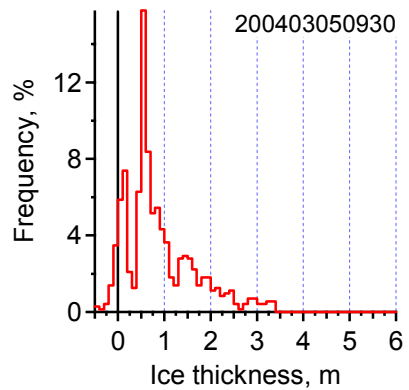
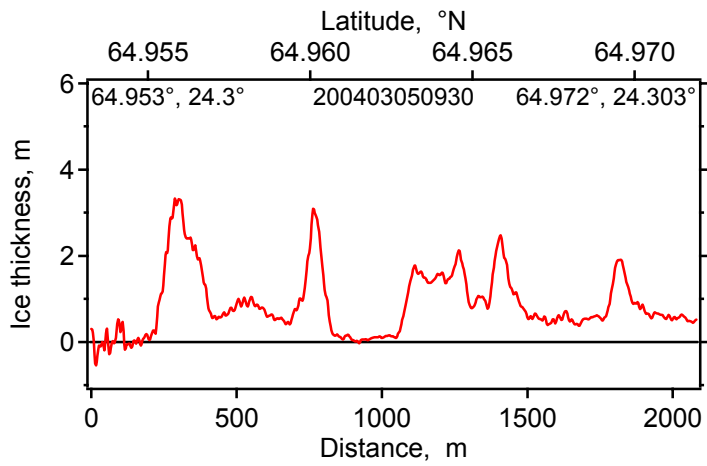
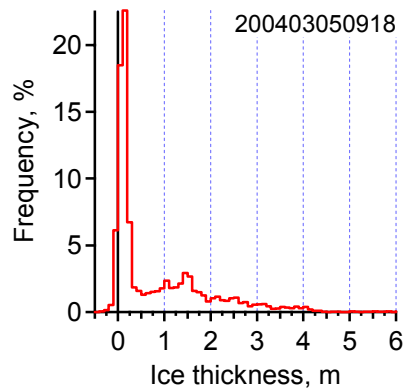
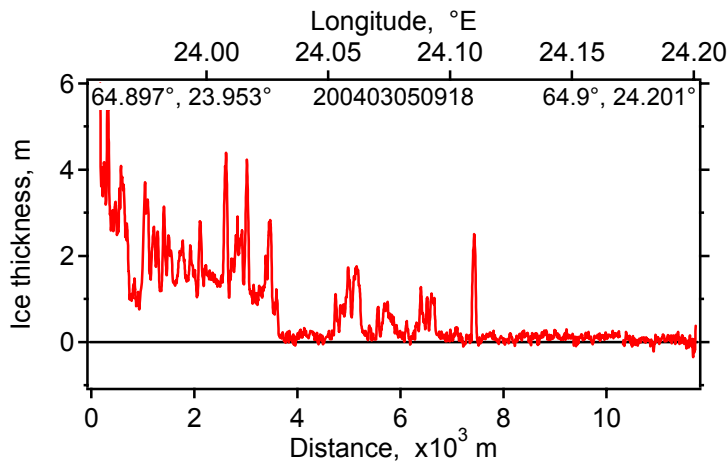
04.3.2004 modified Triangle



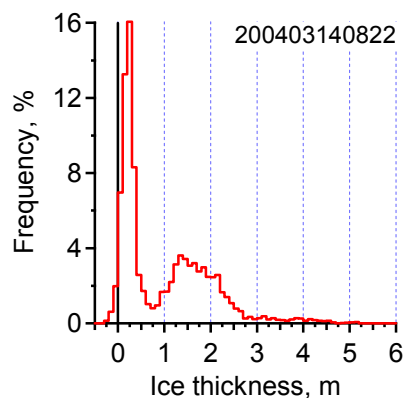
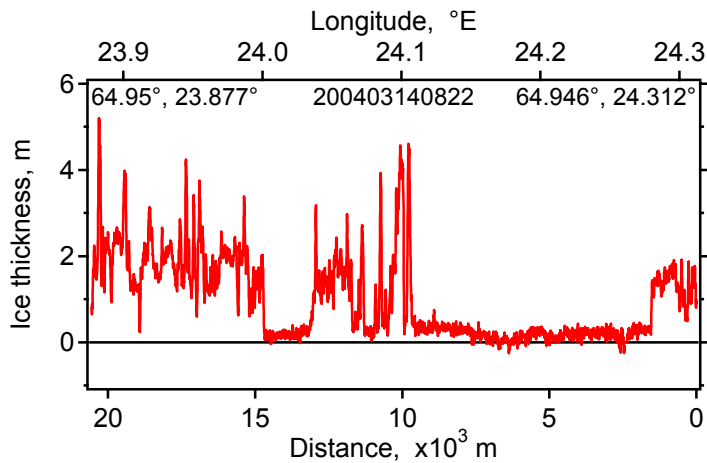
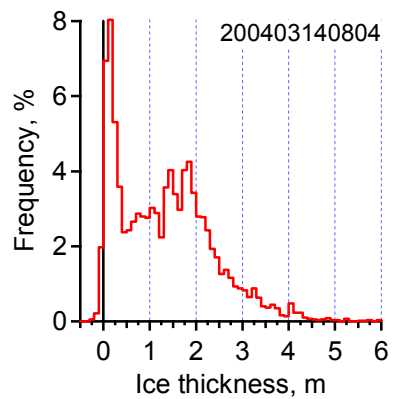
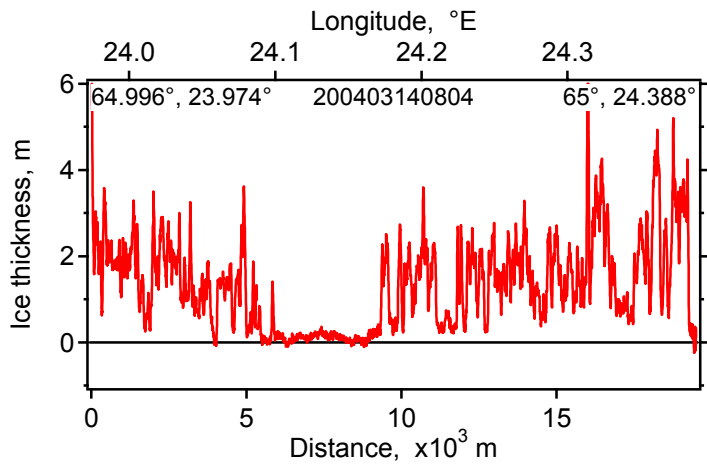
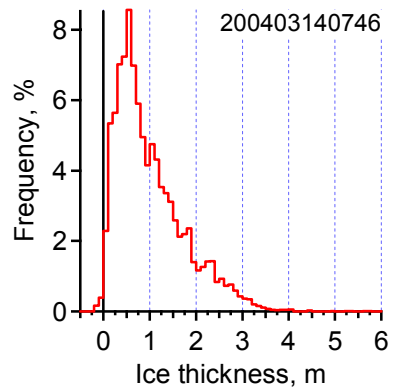
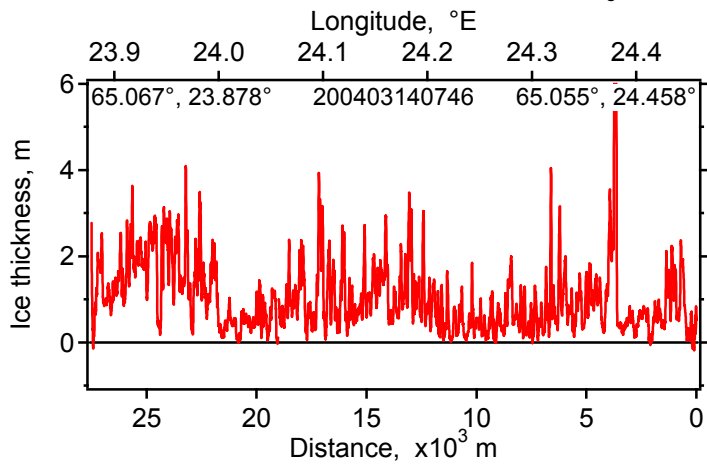
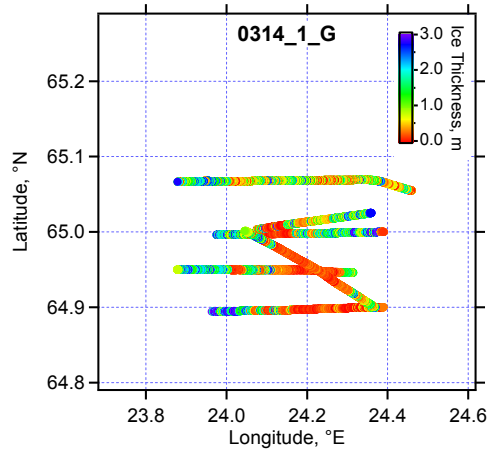


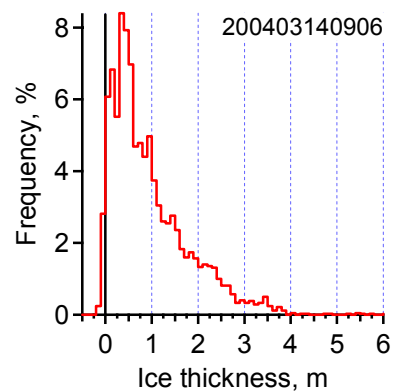
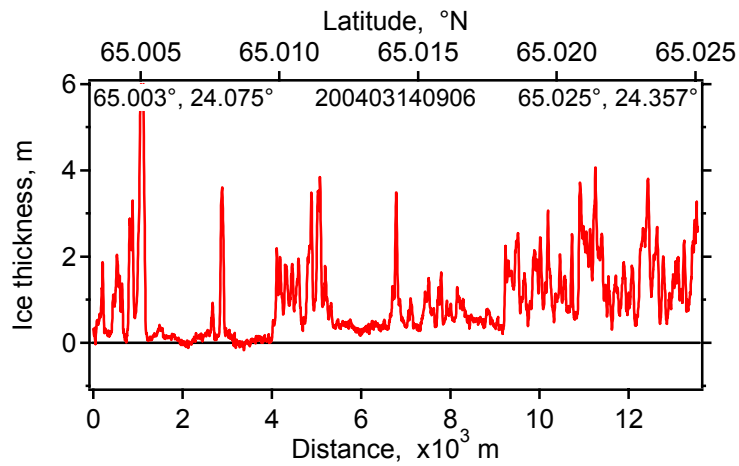
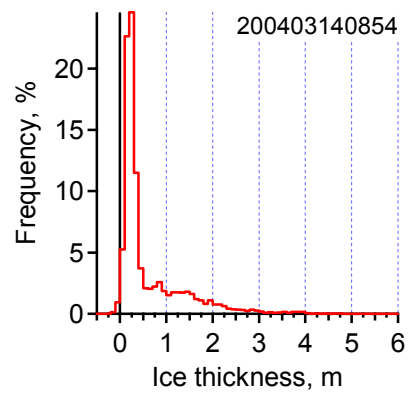
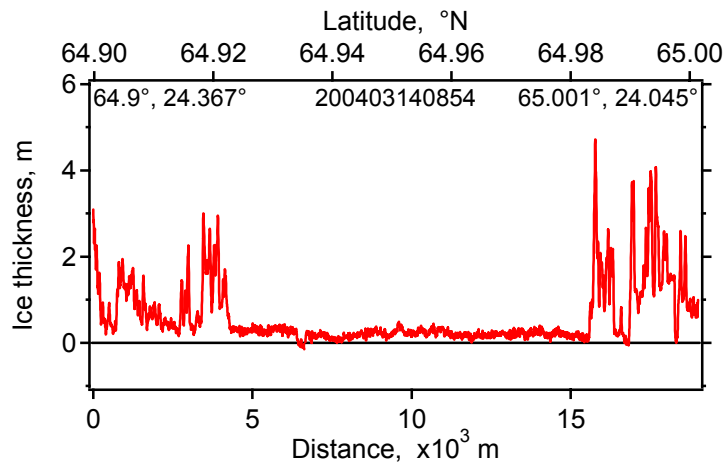
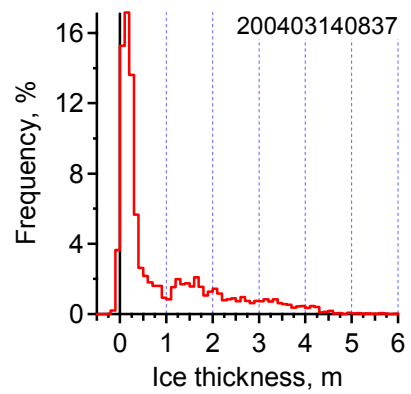
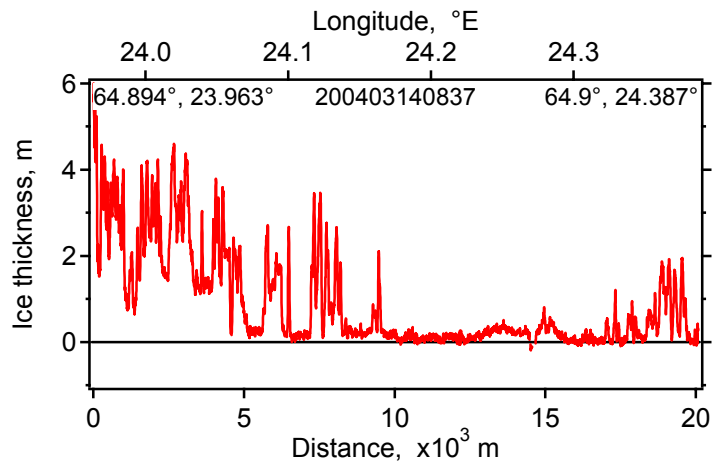
05.3.2004 Grid



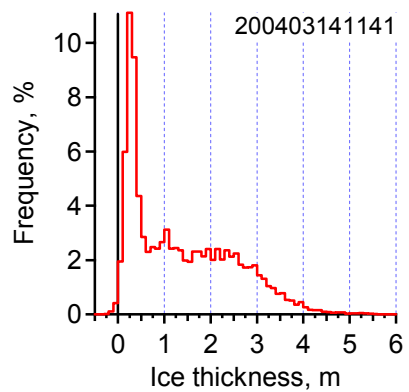
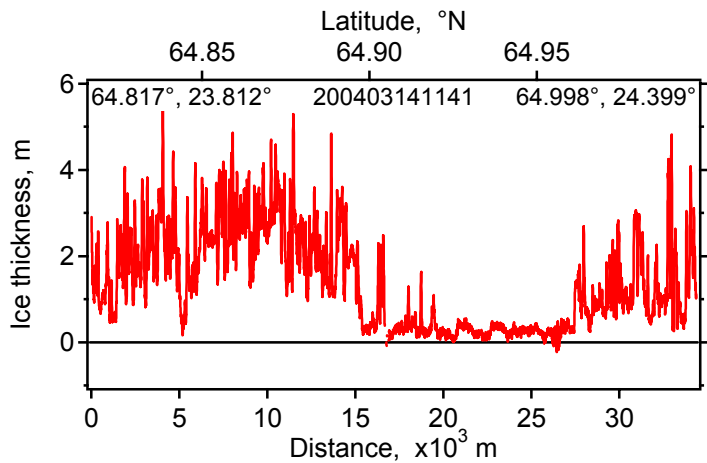
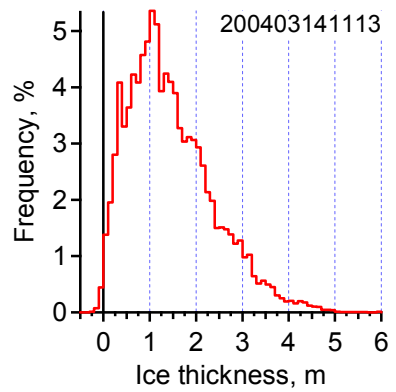
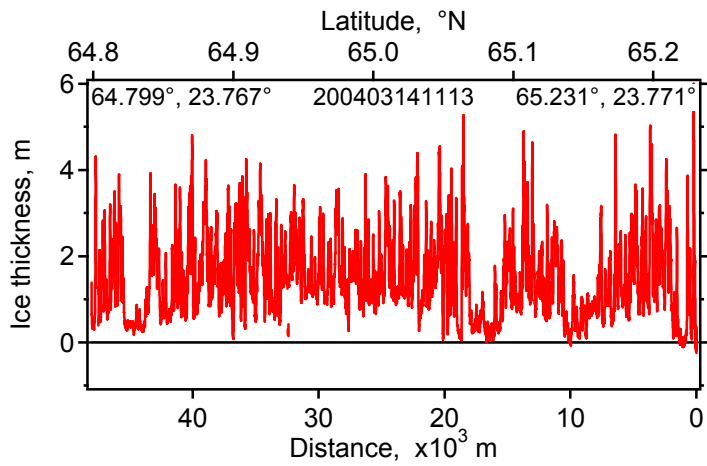
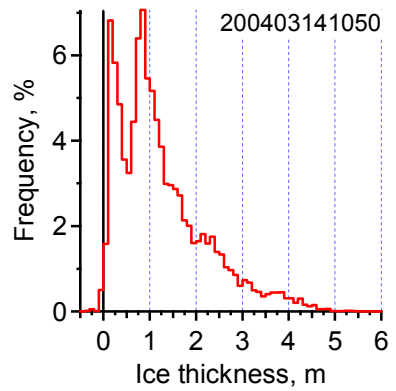
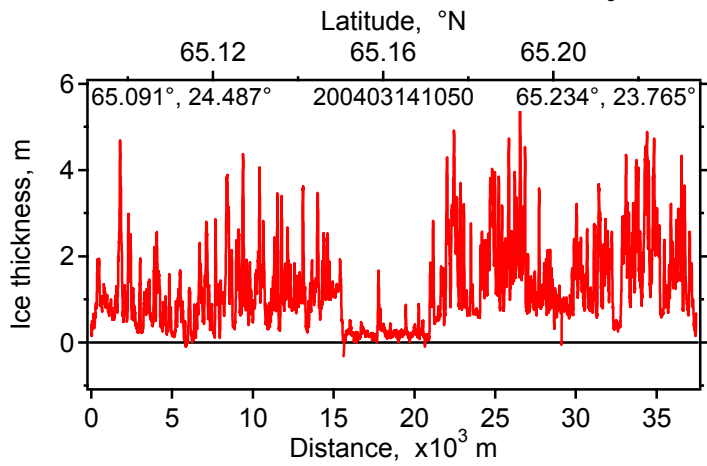
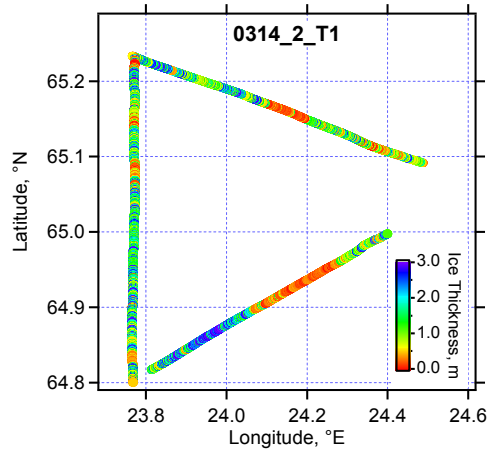


14.3.2004 Grid

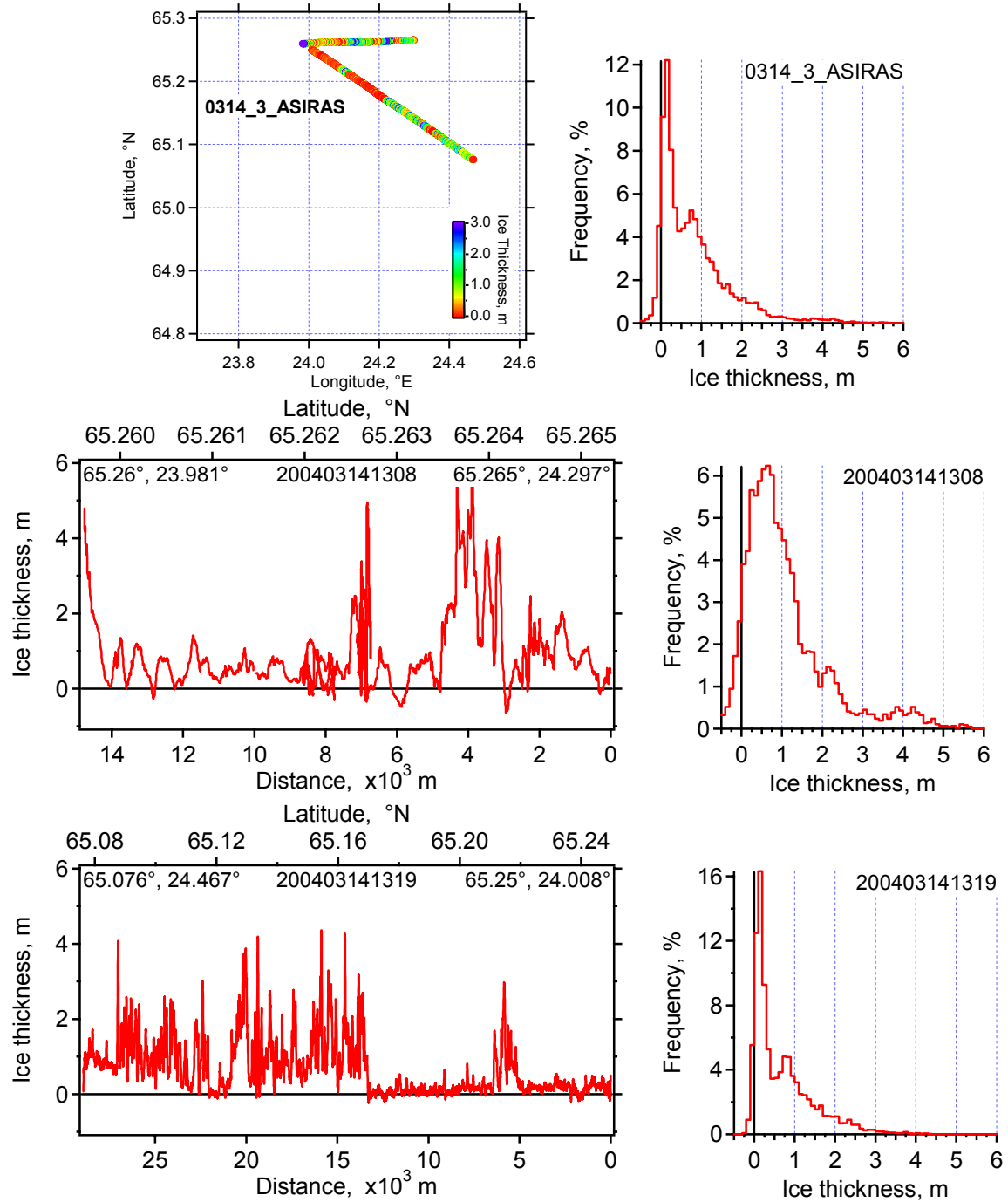




14.3.2004 Triangle



14.3.2004 2 legs for ASIRAS



17.3.2004 ASIRAS fast ice profile

